US011368139B2

(12) **United States Patent**
Garcia

(10) **Patent No.: US 11,368,139 B2**
(45) **Date of Patent: *Jun. 21, 2022**

(54) **SMALL TRANSVERSELY-EXCITED FILM BULK ACOUSTIC RESONATORS WITH ENHANCED Q-FACTOR**

(71) Applicant: **Resonant Inc.**, Austin, TX (US)

(72) Inventor: **Bryant Garcia**, Belmont, CA (US)

(73) Assignee: **Resonant Inc.**, Austin, TX (US)

(*) Notice: Subject to any disclaimer, the term of this patent is extended or adjusted under 35 U.S.C. 154(b) by 2 days.

This patent is subject to a terminal disclaimer.

(21) Appl. No.: **17/460,166**

(22) Filed: **Aug. 28, 2021**

(65) **Prior Publication Data**

US 2021/0391846 A1 Dec. 16, 2021

Related U.S. Application Data

(63) Continuation of application No. 17/229,767, filed on Apr. 13, 2021.

(Continued)

(51) **Int. Cl.**

H03H 9/205	(2006.01)
H03H 9/02	(2006.01)
H03H 9/56	(2006.01)

(52) **U.S. Cl.**

CPC ***H03H 9/205*** (2013.01); ***H03H 9/0211*** (2013.01); ***H03H 9/02015*** (2013.01); ***H03H 9/02228*** (2013.01); ***H03H 9/568*** (2013.01)

(58) **Field of Classification Search**

CPC H03H 9/02015; H03H 9/0211; H03H 9/02228; H03H 9/205; H03H 9/568;

(Continued)

(56) **References Cited**

U.S. PATENT DOCUMENTS

5,204,575 A * 4/1993 Kanda ..... H03H 9/02818 310/313 B

5,446,330 A 8/1995 Eda et al.

(Continued)

FOREIGN PATENT DOCUMENTS

WO	2016017104	2/2016
WO	2018003273	1/2018

OTHER PUBLICATIONS

Buchanan "Ceramic Materials for Electronics" 3rd Edition, first published in 2004 by Marcel Dekker, Inc. pp. 496 (Year 2004).

(Continued)

Primary Examiner — Samuel S Outten

(74) *Attorney, Agent, or Firm* — SoCal IP Law Group LLP; Angelo Gaz

(57) **ABSTRACT**

An acoustic resonator device includes a conductor pattern formed on a surface of a piezoelectric plate. The conductor pattern includes a first busbar, a second busbar, and n interleaved parallel fingers of an interdigital transducer (IDT), where n is a positive integer. The fingers extend alternately from the first and second busbars. A first finger and an n'th finger are at opposing ends of the IDT. The conductor pattern also includes a first reflector element proximate and parallel to the first finger and a second reflector element proximate and parallel to the n'th finger. A center-to-center distance pr between the first reflector element and the first finger and between the second reflector element and the n'th finger is greater than or equal to 1.2 times a pitch p of the IDT and less than or equal to 1.5 times the pitch p.

17 Claims, 13 Drawing Sheets

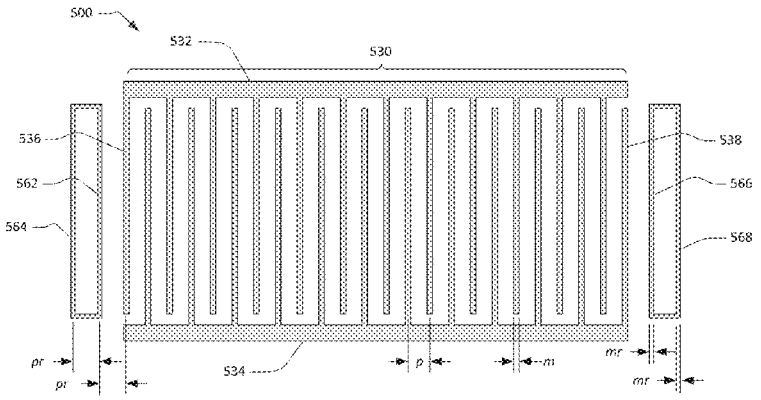

Related U.S. Application Data

(60) Provisional application No. 63/012,849, filed on Apr. 20, 2020, provisional application No. 63/066,520, filed on Aug. 17, 2020, provisional application No. 63/074,991, filed on Sep. 4, 2020.

(58) **Field of Classification Search**
CPC H03H 9/02685; H03H 9/02803; H03H 9/02866; H03H 9/0504; H03H 9/173; H03H 9/174
USPC ..... 333/195; 310/313 D
See application file for complete search history.

(56) **References Cited**

U.S. PATENT DOCUMENTS

5,552,655	A	9/1996	Stokes et al.	
5,631,515	A *	5/1997	Mineyoshi	H03H 9/02866 310/313 B
5,726,610	A	3/1998	Allen et al.	
5,729,186	A *	3/1998	Seki	H03H 9/6483 310/313 A
5,853,601	A	12/1998	Krishaswamy	
6,172,582	B1 *	1/2001	Hickernell	H03H 9/25 310/313 D
6,271,617	B1 *	8/2001	Yoneda	H03H 9/6483 310/313 D
6,377,140	B1	4/2002	Ehara et al.	
6,516,503	B1	2/2003	Ikada et al.	
6,540,827	B1	4/2003	Levy et al.	
6,570,470	B2 *	5/2003	Maehara	H03H 9/6483 310/313 B
6,707,229	B1	3/2004	Martin	
6,710,514	B2	3/2004	Ikada et al.	
6,833,774	B2 *	12/2004	Abbott	H03H 9/6483 310/313 A
7,009,468	B2 *	3/2006	Kadota	H03H 9/02551 310/313 B
7,345,400	B2	3/2008	Nakao et al.	
7,463,118	B2	12/2008	Jacobsen	
7,535,152	B2	5/2009	Ogami et al.	
7,684,109	B2	3/2010	Godshalk et al.	
7,728,483	B2	6/2010	Tanaka	
7,868,519	B2	1/2011	Umeda	
7,941,103	B2	5/2011	Iwamoto et al.	
7,965,015	B2	6/2011	Tai et al.	
8,278,802	B1	10/2012	Lee et al.	
8,294,330	B1	10/2012	Abbott et al.	
8,344,815	B2	1/2013	Yamanaka et al.	
8,816,567	B2	8/2014	Zuo et al.	
8,829,766	B2	9/2014	Milyutin et al.	
8,932,686	B2	1/2015	Hayakawa et al.	
9,093,979	B2	7/2015	Wang	
9,112,134	B2	8/2015	Takahashi	
9,130,145	B2	9/2015	Martin et al.	
9,148,121	B2 *	9/2015	Inoue	H03H 9/14538
9,219,466	B2	12/2015	Meltaus et al.	
9,276,557	B1	3/2016	Nordquist et al.	
9,369,105	B1	6/2016	Li et al.	
9,425,765	B2	8/2016	Rinaldi	
9,525,398	B1	12/2016	Olsson	
9,640,750	B2	5/2017	Nakanishi et al.	
9,748,923	B2	8/2017	Kando et al.	
9,762,202	B2	9/2017	Thalmayr et al.	
9,780,759	B2	10/2017	Kimura et al.	
9,837,984	B2	12/2017	Khlat et al.	
10,079,414	B2	9/2018	Guyette et al.	
10,187,039	B2	1/2019	Komatsu et al.	
10,200,013	B2	2/2019	Bower et al.	
10,211,806	B2	2/2019	Bhattacharjee	
10,284,176	B1	5/2019	Solal	
10,491,192	B1	11/2019	Plesski et al.	
10,601,392	B2	3/2020	Plesski et al.	
10,637,438	B2	4/2020	Garcia et al.	
10,644,674	B2	5/2020	Takamine	
10,756,697	B2	8/2020	Plesski et al.	
10,790,802	B2	9/2020	Yantchev et al.	
10,797,675	B2	10/2020	Plesski	
10,812,048	B2 *	10/2020	Nosaka	H03H 9/6403
10,819,309	B1	10/2020	Turner et al.	
10,826,462	B2	11/2020	Plesski et al.	
10,868,510	B2	12/2020	Yantchev et al.	
10,868,512	B2	12/2020	Garcia et al.	
10,868,513	B2	12/2020	Yantchev	
10,911,017	B2	2/2021	Plesski	
10,911,021	B2	2/2021	Turner et al.	
10,911,023	B2	2/2021	Turner	
10,917,070	B2	2/2021	Plesski et al.	
10,917,072	B2	2/2021	McHugh et al.	
10,985,726	B2	4/2021	Plesski	
10,985,728	B2	4/2021	Plesski et al.	
10,985,730	B2	4/2021	Garcia	
10,992,282	B1	4/2021	Plesski et al.	
10,992,283	B2	4/2021	Plesski et al.	
10,992,284	B2	4/2021	Yantchev	
10,998,877	B2	5/2021	Turner et al.	
10,998,882	B2	5/2021	Yantchev et al.	
11,003,971	B2	5/2021	Plesski et al.	
2002/0079986	A1	6/2002	Ruby et al.	
2002/0158714	A1	10/2002	Kaitila et al.	
2002/0189062	A1	12/2002	Lin et al.	
2003/0042998	A1 *	3/2003	Edmonson	H03H 9/25 333/195
2003/0080831	A1	5/2003	Naumenko et al.	
2003/0199105	A1	10/2003	Kub et al.	
2004/0100164	A1	5/2004	Murata	
2004/0261250	A1	12/2004	Kadota et al.	
2005/0077982	A1 *	4/2005	Funasaka	H03H 9/02574 333/195
2005/0185026	A1	8/2005	Noguchi et al.	
2005/0218488	A1	10/2005	Matsuo	
2005/0264136	A1	12/2005	Tsutsumi et al.	
2006/0152107	A1 *	7/2006	Tanaka	H03H 9/02551 310/313 R
2006/0179642	A1	8/2006	Kawamura	
2007/0182510	A1	8/2007	Park	
2007/0188047	A1	8/2007	Tanaka	
2007/0194863	A1	8/2007	Shibata et al.	
2007/0267942	A1	11/2007	Matsumoto et al.	
2008/0246559	A1	10/2008	Ayazi	
2010/0064492	A1	3/2010	Tanaka	
2010/0123367	A1	5/2010	Tai et al.	
2011/0018389	A1	1/2011	Fukano et al.	
2011/0018654	A1	1/2011	Bradley et al.	
2011/0109196	A1	5/2011	Goto et al.	
2011/0278993	A1	11/2011	Iwamoto	
2012/0073390	A1 *	3/2012	Zaghloul	G01N 29/022 73/865
2012/0286900	A1	11/2012	Kadota et al.	
2013/0127554	A1 *	5/2013	Yamanaka	H03H 9/643 331/155
2013/0234805	A1	9/2013	Takahashi	
2013/0271238	A1	10/2013	Onda	
2013/0278609	A1	10/2013	Stephanou et al.	
2013/0321100	A1	12/2013	Wang	
2014/0130319	A1	5/2014	Iwamoto	
2014/0145556	A1	5/2014	Kadota	
2014/0151151	A1	6/2014	Reinhardt	
2014/0152145	A1	6/2014	Kando et al.	
2014/0173862	A1	6/2014	Kando et al.	
2014/0225684	A1	8/2014	Kando et al.	
2015/0042417	A1	2/2015	Onodera et al.	
2015/0165479	A1	6/2015	Lasiter et al.	
2015/0319537	A1	11/2015	Perois et al.	
2015/0333730	A1	11/2015	Meltaus et al.	
2016/0028367	A1	1/2016	Shealy	
2016/0182009	A1	6/2016	Bhattacharjee	
2017/0063332	A1	3/2017	Gilbert et al.	
2017/0179225	A1	6/2017	Kishimoto	
2017/0179928	A1	6/2017	Raihn et al.	
2017/0214381	A1	7/2017	Bhattacharjee	
2017/0214387	A1	7/2017	Burak et al.	
2017/0222617	A1	8/2017	Mizoguchi	
2017/0222622	A1	8/2017	Solal et al.	

(56) **References Cited**

U.S. PATENT DOCUMENTS

2017/0370791	A1	12/2017	Nakamura et al.	
2018/0005950	A1	1/2018	Watanabe	
2018/0026603	A1	1/2018	Iwamoto	
2018/0033952	A1	2/2018	Yamamoto	
2018/0041191	A1	2/2018	Park	
2018/0062615	A1	3/2018	Kato et al.	
2018/0062617	A1	3/2018	Yun et al.	
2018/0123016	A1	5/2018	Gong	
2018/0191322	A1	7/2018	Chang et al.	
2018/0278227	A1	9/2018	Hurwitz	
2019/0068164	A1	2/2019	Houlden et al.	
2019/0123721	A1	4/2019	Takamine	
2019/0131953	A1	5/2019	Gong	
2019/0273480	A1	9/2019	Lin et al.	
2019/0348966	A1	11/2019	Campanella-Pineda	
2019/0379351	A1*	12/2019	Miyamoto	H03H 9/547
2019/0386636	A1	12/2019	Plesski et al.	
2020/0007110	A1*	1/2020	Konaka	H03H 9/02637
2020/0021272	A1*	1/2020	Segovia Fernandez	H03B 5/364
2020/0036357	A1	1/2020	Mimura	
2020/0235719	A1	7/2020	Yantchev et al.	
2020/0350891	A1	11/2020	Turner	
2021/0013859	A1	1/2021	Turner et al.	
2021/0328574	A1*	10/2021	Garcia	H03H 9/568

OTHER PUBLICATIONS

Sorokin et al. Study of Microwave Acoustic Attenuation in a Multi-frequency Bulk Acoustic Resonator Based on a Synthetic Diamond Single Crystal Published in Acoustical Physics, vol. 61, No. 6, 2015 pp. 675 (Year 2015) 00 Jan. 2015.

Zou, Jie "High-Performance Aluminum Nitride Lamb Wave Resonators for RF Front-End Technology" University of California, Berkeley, Summer 2015, pp. 63 (Year 2015) 00 Jan. 2015.

Santosh, G. , Surface acoustic wave devices on silicon using patterned and thin film ZnO, Ph.D. thesis, Feb. 2016, Indian Institute of technology Guwahati, Assam, India Feb. 2016.

Merriam Webster, dictionary meaning of the word "diaphragm", since 1828, Merriam Webster (Year: 1828) 1828.

Kadota et al. "5.4 Ghz Lamb Wave Resonator on LiNbO3 Thin Crystal Plate and Its Application," published in Japanese Journal of Applied Physics 50 (2011) 07HD11. (Year: 2011) 2011.

Safari et al. "Piezoelectric for Transducer Applications" published by Elsevier Science Ltd., pp. 4 (Year: 2000). 2020.

Moussa et al. Review on Triggered Liposomal Drug Delivery with a Focus on Ultrasound 2015, Bentham Science Publishers, pp. 16 (Year 2005) 2005.

Acoustic Properties of Solids ONDA Corporation 592 Weddell Drive, Sunnyvale, CA 94089, Apr. 11, 2003, pp. 5 (Year 2003). 2003.

Bahreyni, B. Fabrication and Design of Resonant Microdevices Andrew William, Inc. 2018, NY (Year 2008). 2008.

Material Properties of Tibtech Innovations, © 2018 Tibtech Innovations (Year 2018). 2018.

USPTO/ISA, International Search Report and Written Opinion for PCT Application No. PCT/US2020/45654 dated Oct. 29, 2020.

T. Takai, H. Iwamoto, et al., "I.H.P.Saw Technology and its Application to Microacoustic Components (Invited)." 2017 IEEE International Ultrasonics Symposium, Sep. 6-9, 2017. pp. 1-8.

R. Olsson III, K. Hattar et al. "A high electromechanical coupling coefficient SH0 Lamb wave lithiumniobate micromechanical resonator and a method for fabrication" Sensors and Actuators A: Physical, vol. 209, Mar. 1, 2014, pp. 183-190.

M. Kadota, S. Tanaka, "Wideband acoustic wave resonators composed of hetero acoustic layer structure," Japanese Journal of Applied Physics, vol. 57, No. 7S1. Published Jun. 5, 2018. 5 pages.

Y. Yang, R. Lu et al. "Towards Ka Band Acoustics: Lithium Niobat Asymmetrical Mode Piezoelectric MEMS Resonators", Department of Electrical and Computer Engineering University of Illinois at Urbana-Champaign, May 2018. pp. 1-2.

Y. Yang, A. Gao et al. "5 GHZ Lithium Niobate MEMS Resonators With High FOM of 153", 2017 IEEE 30th International Conference in Micro Electro Mechanical Systems (MEMS). Jan. 22-26, 2017. pp. 942-945.

USPTO/ISA, International Search Report and Written Opinion for PCT Application No. PCT/US2019/036433 dated Aug. 29, 2019.

USPTO/ISA, International Search Report and Written Opinion for PCT Application No. PCT/US2019/058632 dated Jan. 17, 2020.

G. Manohar, "Investigation of Various Surface Acoustic Wave Design Configurations for Improved Sensitivity." Doctoral dissertation, University of South Florida, USA, Jan. 2012, 7 pages.

Ekeom, D. & Dubus, Bertrand & Volatier, A . . . (2006). Solidly mounted resonator (SMR) FEM-BEM simulation. 1474-1477. 10.1109/ULTSYM.2006.371.

Mizutaui, K. and Toda, K., "Analysis of lamb wave propagation characteristics in rotated Ycut Xpropagation LiNbO3 plates." Electron. Comm. Jpn. Pt. I, 69, No. 4 (1986): 47-55. doi:10.1002/ecja.4410690406.

Naumenko et al., "Optimal orientations of Lithium Niobate for resonator SAW filters", 2003 IEEE Ultrasonics Symposium—pp. 2110-2113. (Year: 2003).

Namdeo et al. "Simulation on Effects of Electrical Loading due to Interdigital Transducers in Surface Acoustic Wave Resonator", published in Procedia Engineering 64 (2013) of Science Direct pp. 322-330 (Year: 2013) 2013.

Rodriguez-Madrid et al., "Super-High-Frequency SAW Resonators on AIN/Diamond", IEEE Electron Device Letters, vol. 33, No. 4, Apr. 2012, pp. 495-497. Year: 2012) 2012.

A. C. Guyette, "Theory and Design of Intrinsically Switched Multiplexers With Optimum Phase Linearity," in IEEE Transactions on Microwave Theory and Techniques, vol. 61, No. 9, pp. 3254-3264, Sep. 2013, doi: 10.1109/TMTT.2013.2274963. Sep. 2013.

Yanson Yang, Ruochen Lu, Songbin Gong, High Q Antisymmetric Mode Lithium Niobate MEMS Resonators With Spurious Mitigation, Journal of Microelectromechanical Systems, vol. 29, No. 2, Apr. 2020. Apr. 2, 2020.

Yu-Po Wong, Luyan Qiu, Naoto Matsuoka, Ken-ya Hashimoto, Broadband Piston Mode Operation for First-order Antisymmetric Mode Resonators, 2020 IEEE International Ultrasonics Symposium, Sep. 2020. Sep. 2020.

USPTO/ISA, International Search Report and Written Opinion for PCT Application No. PCT/US2021/024824 dated Jul. 27, 2021, 9 total pages.

* cited by examiner

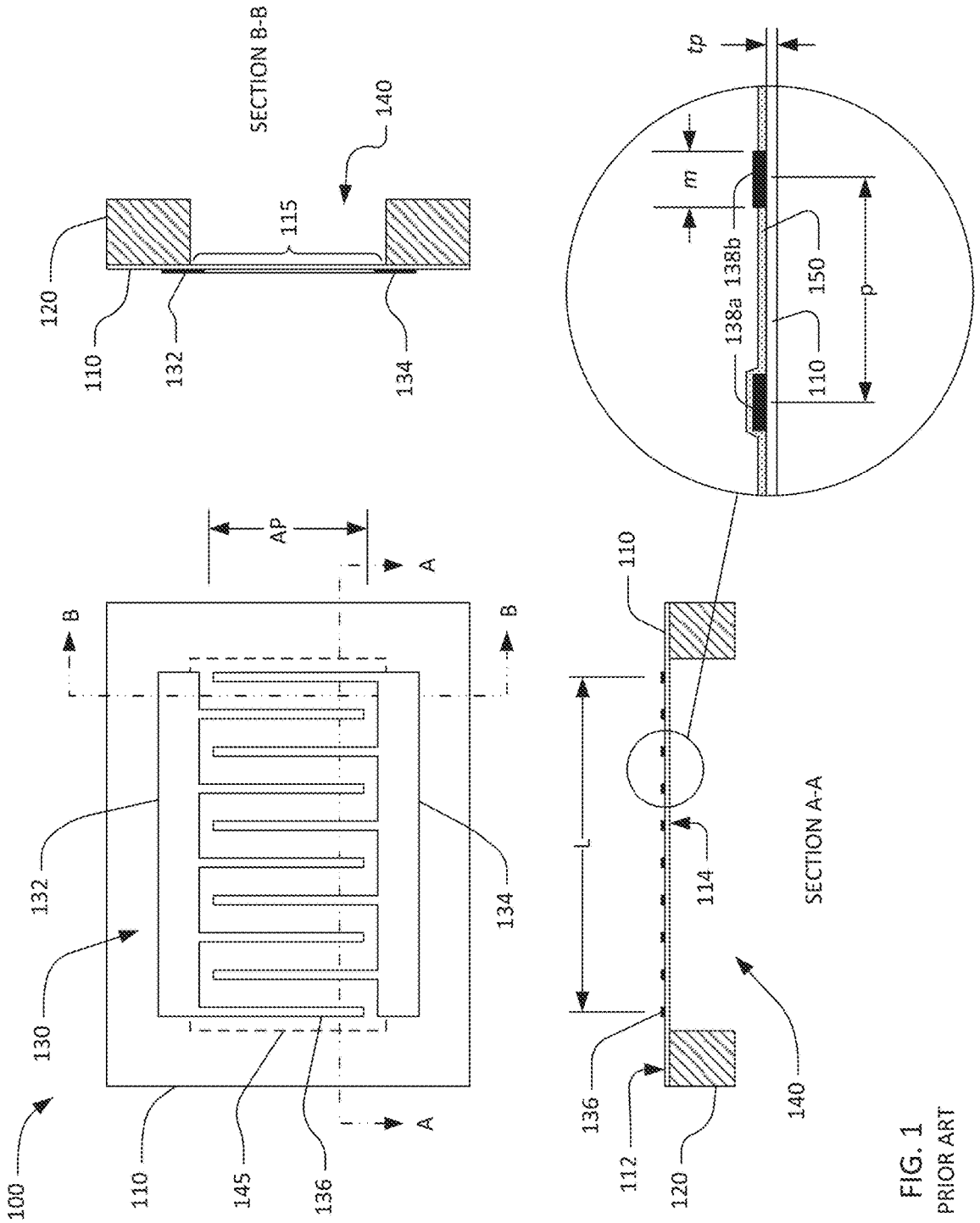

FIG. 1
PRIOR ART

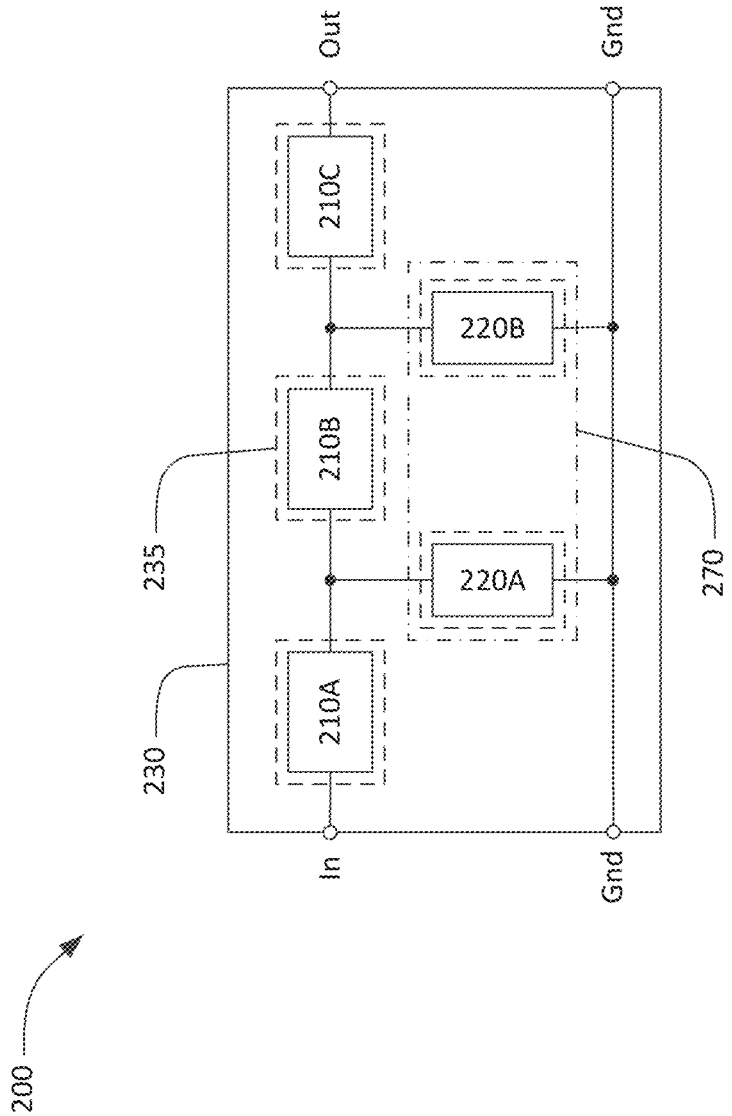

FIG. 2
PRIOR ART

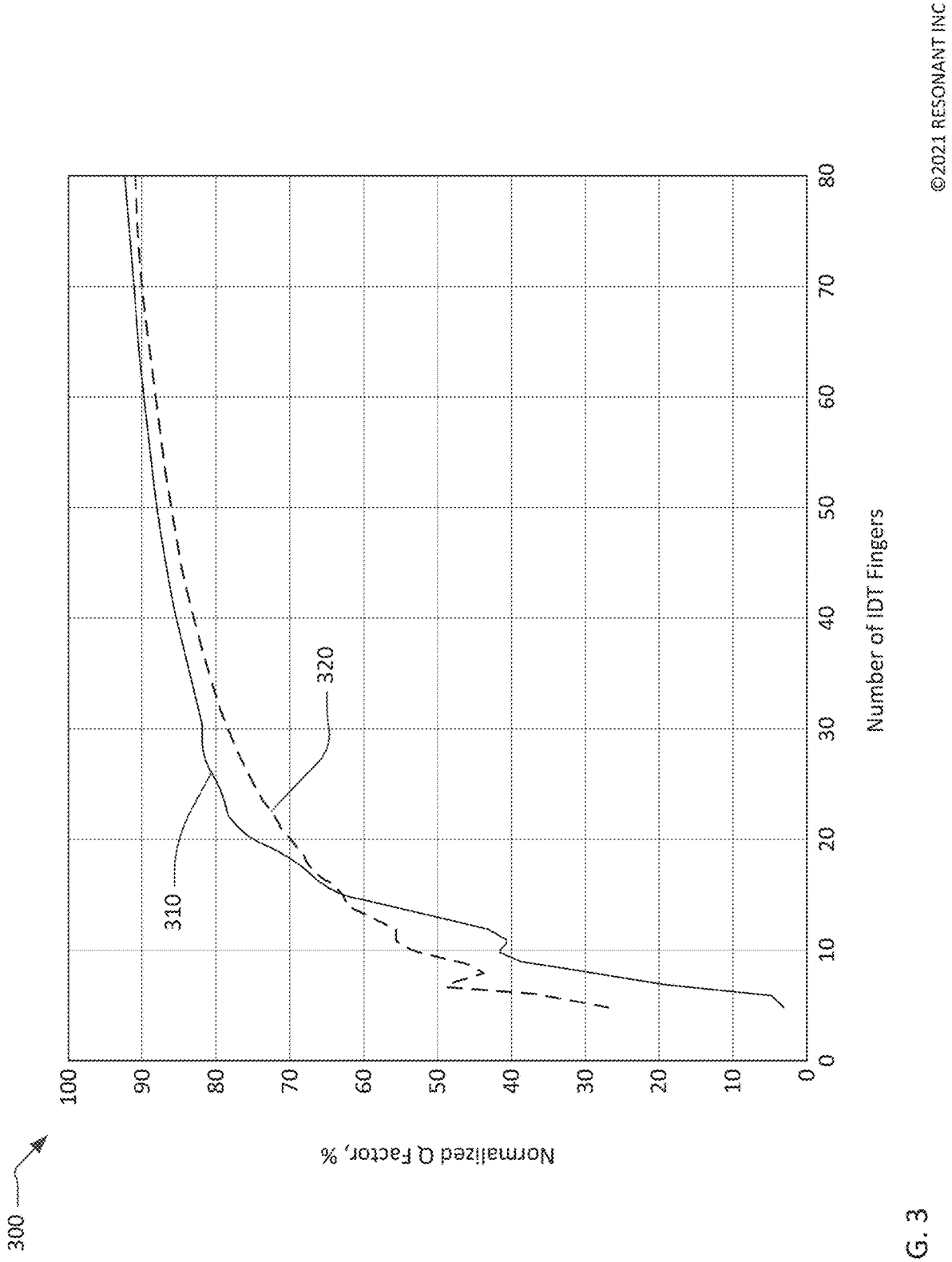
300
Normalized Q Factor, %
100
90
80
70
60
50
40
30
20
10
0
0
10
20
30
40
50
60
70
80
Number of IDT Fingers
310
320
©2021 RESONANT INC

FIG. 3

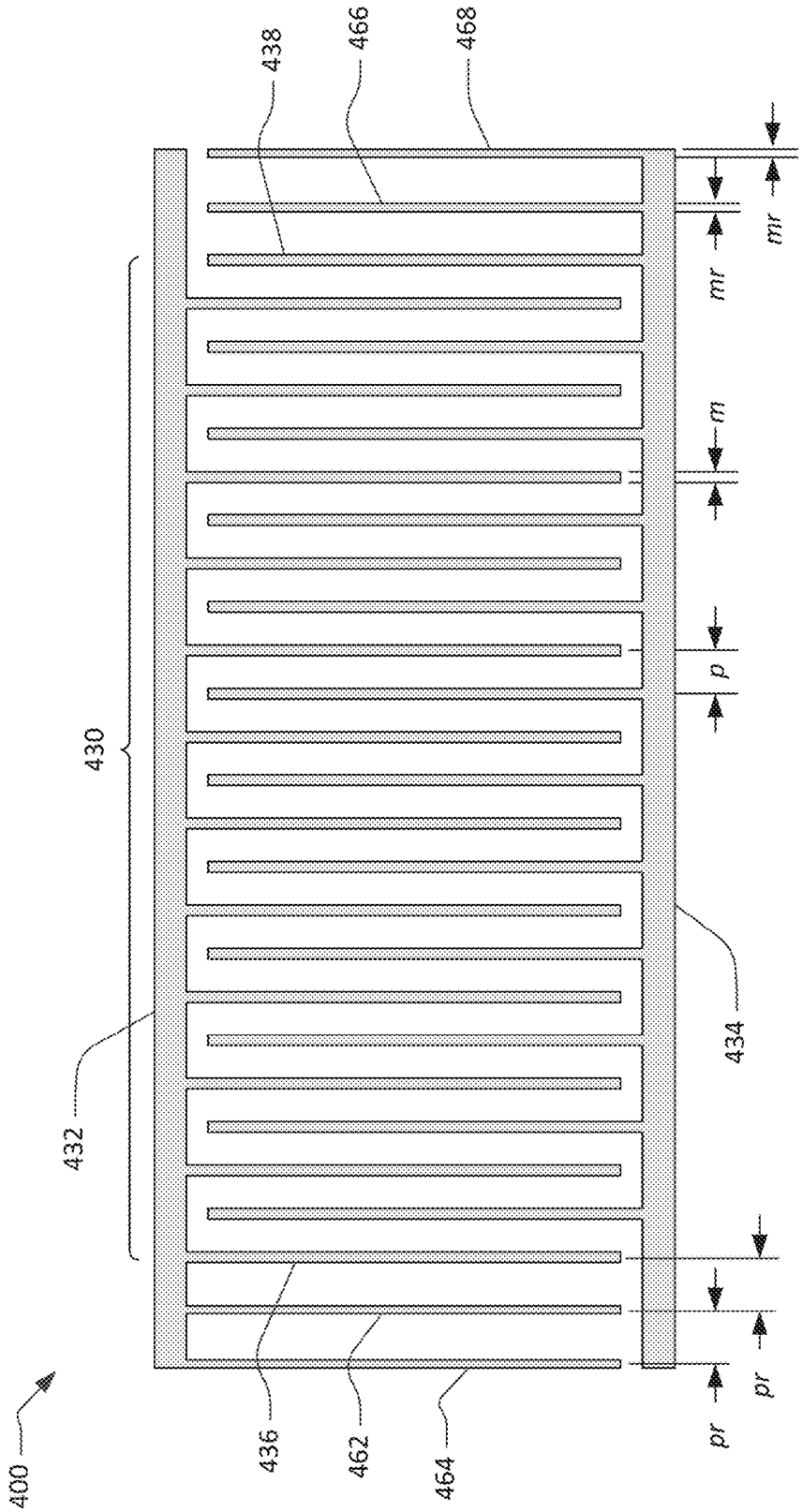

FIG. 4

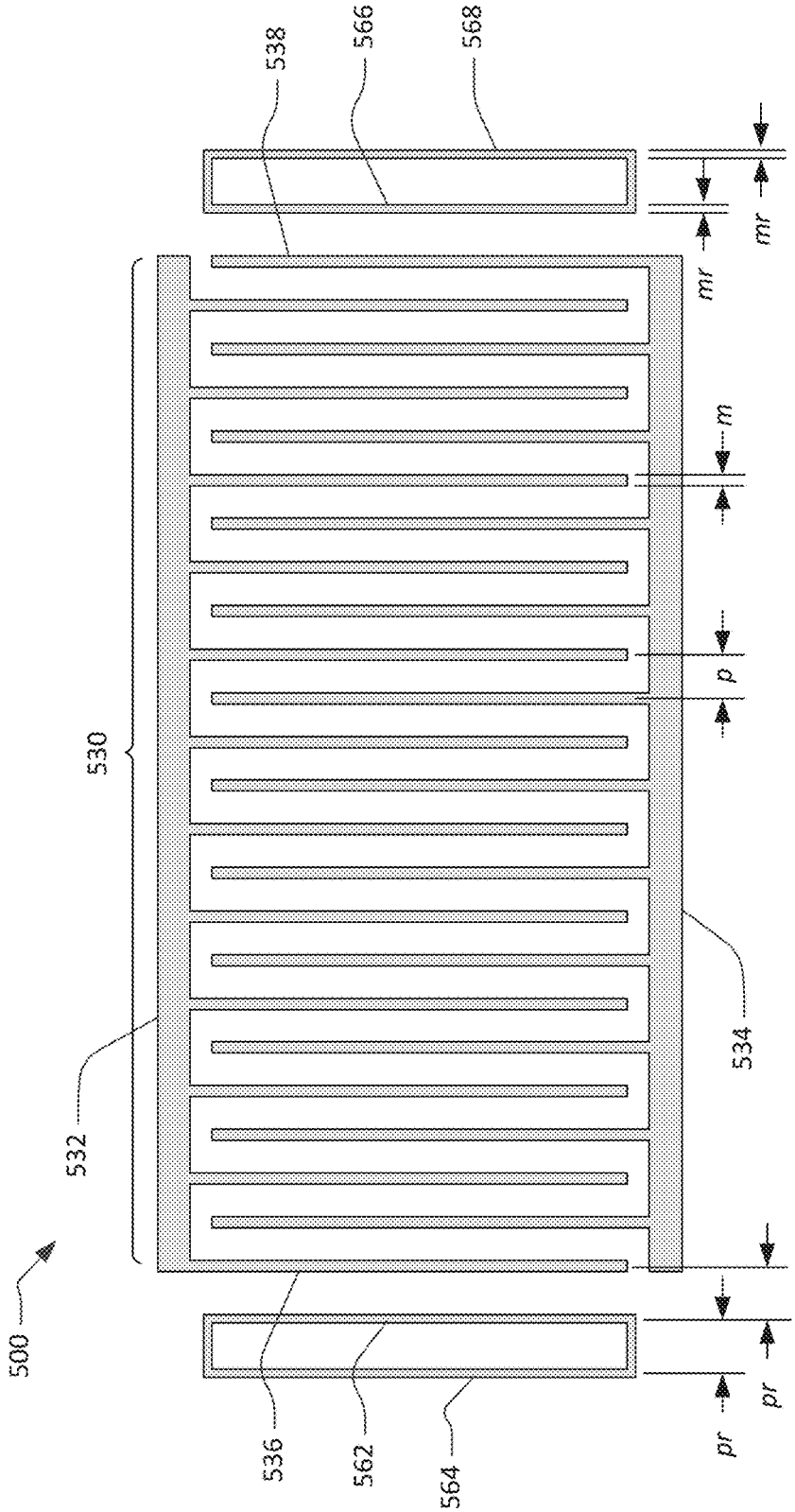

FIG. 5

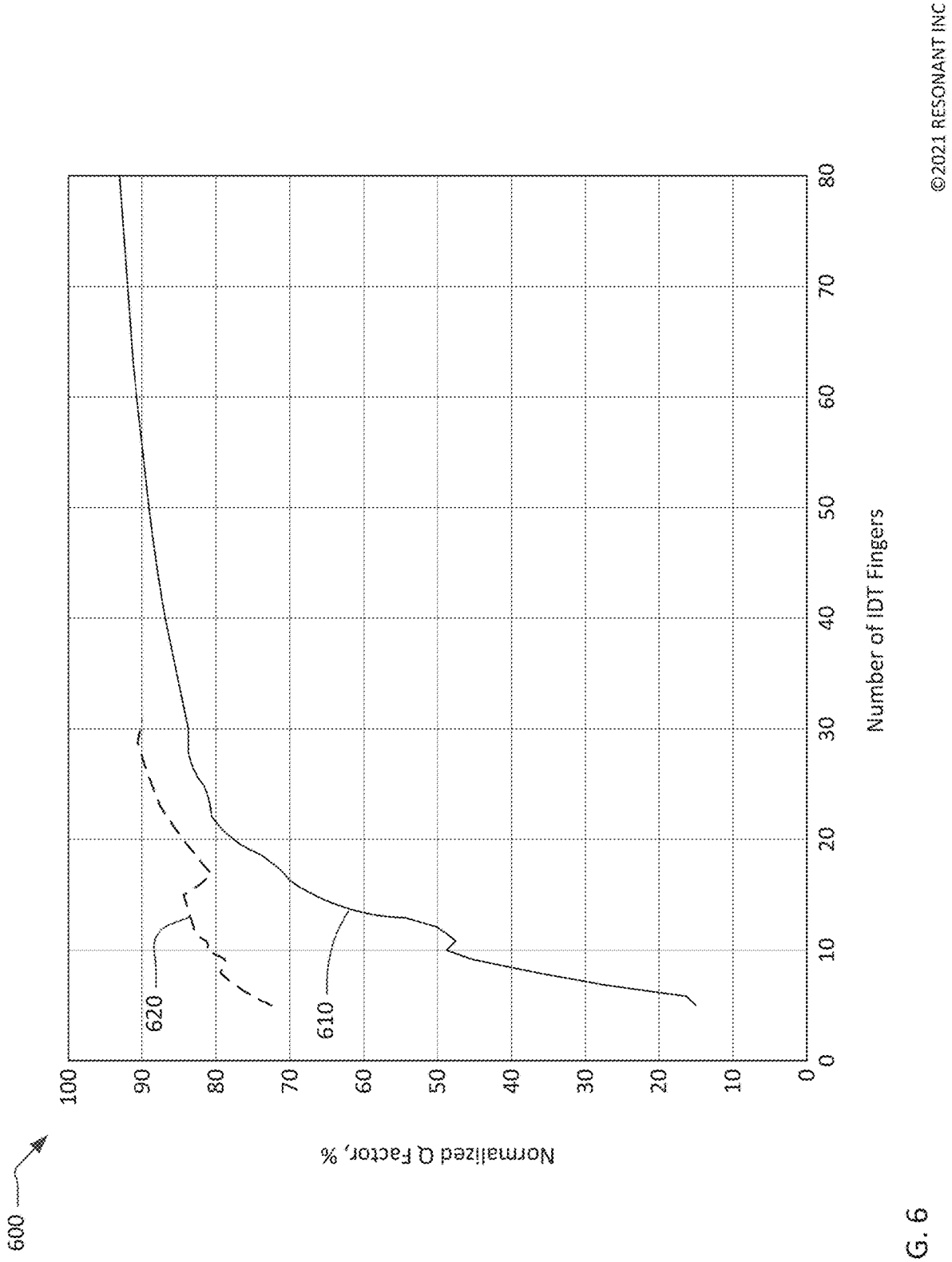
600
Normalized Q Factor, %
100
90
80
70
60
50
40
30
20
10
0
620
610
0
10
20
30
40
50
60
70
80
Number of IDT Fingers
©2021 RESONANT INC

FIG. 6

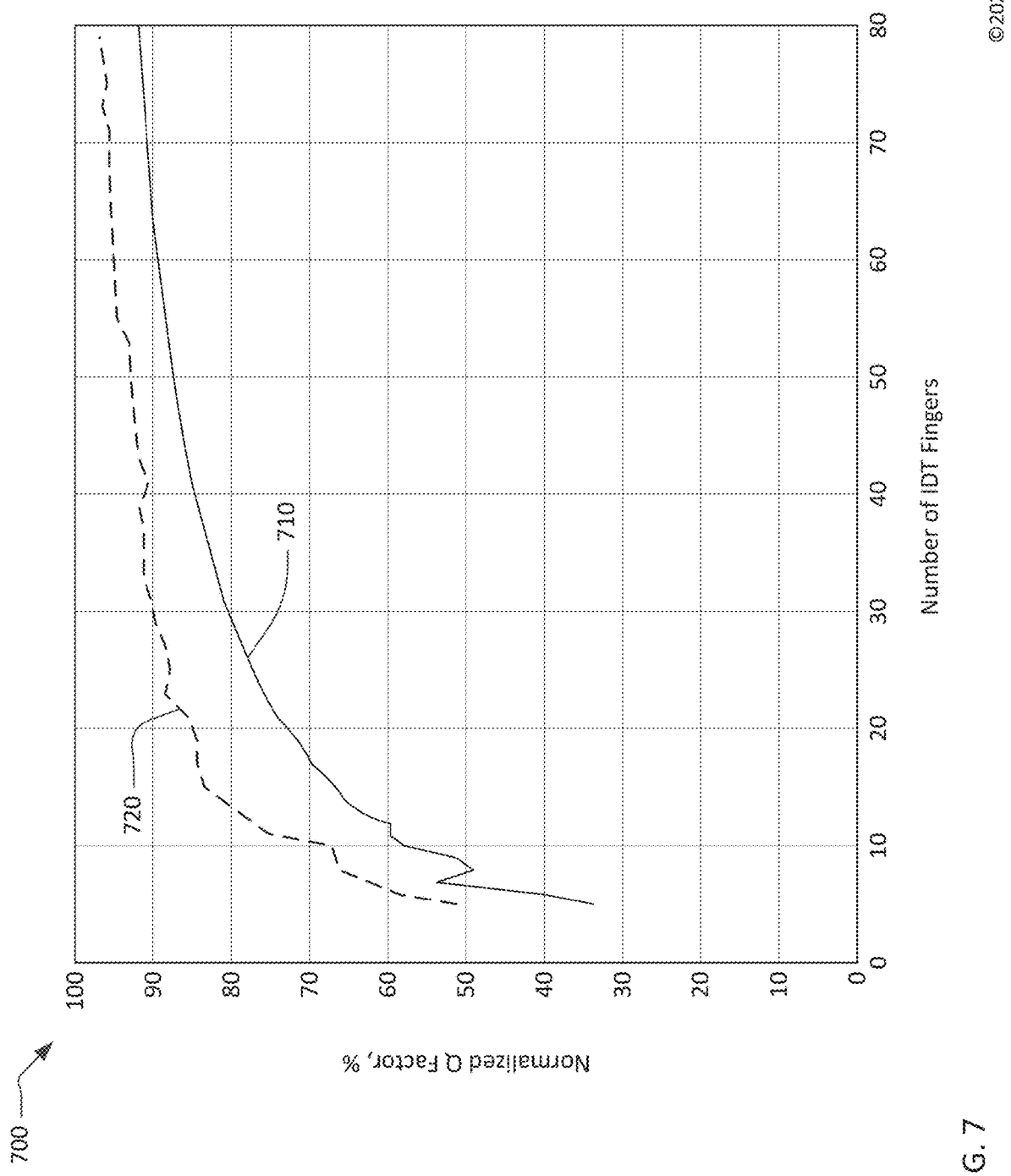
700
Normalized Q Factor, %
100
90
80
70
60
50
40
30
20
10
0
0
10
20
30
40
50
60
70
80
Number of IDT Fingers
710
720
©2021 RESONANT INC

FIG. 7

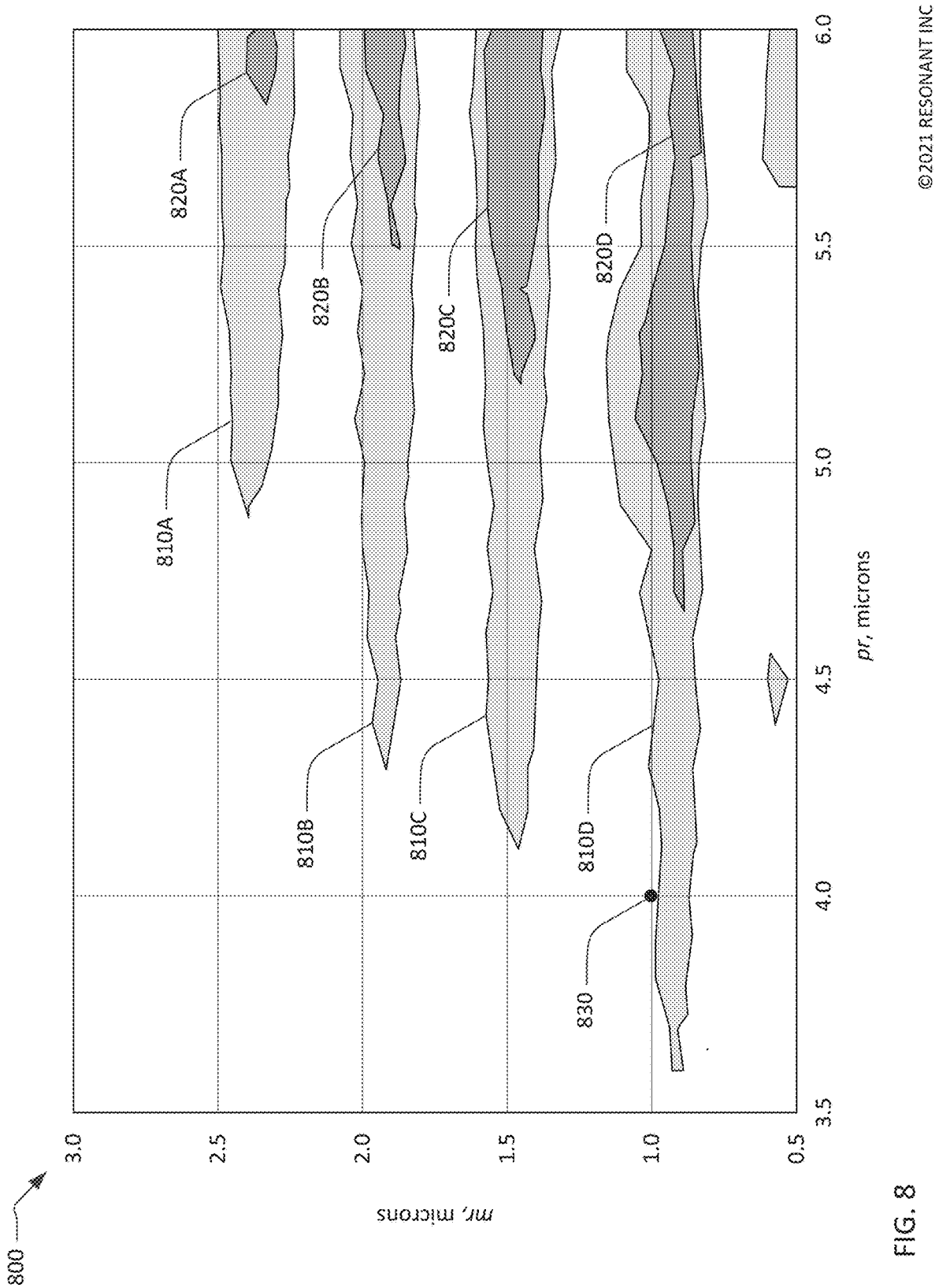
800
3.0
2.5
2.0
1.5
1.0
0.5
mr, microns
3.5
4.0
4.5
5.0
5.5
6.0
pr, microns
820A
820B
820C
820D
810A
810B
810C
810D
830
©2021 RESONANT INC

FIG. 8

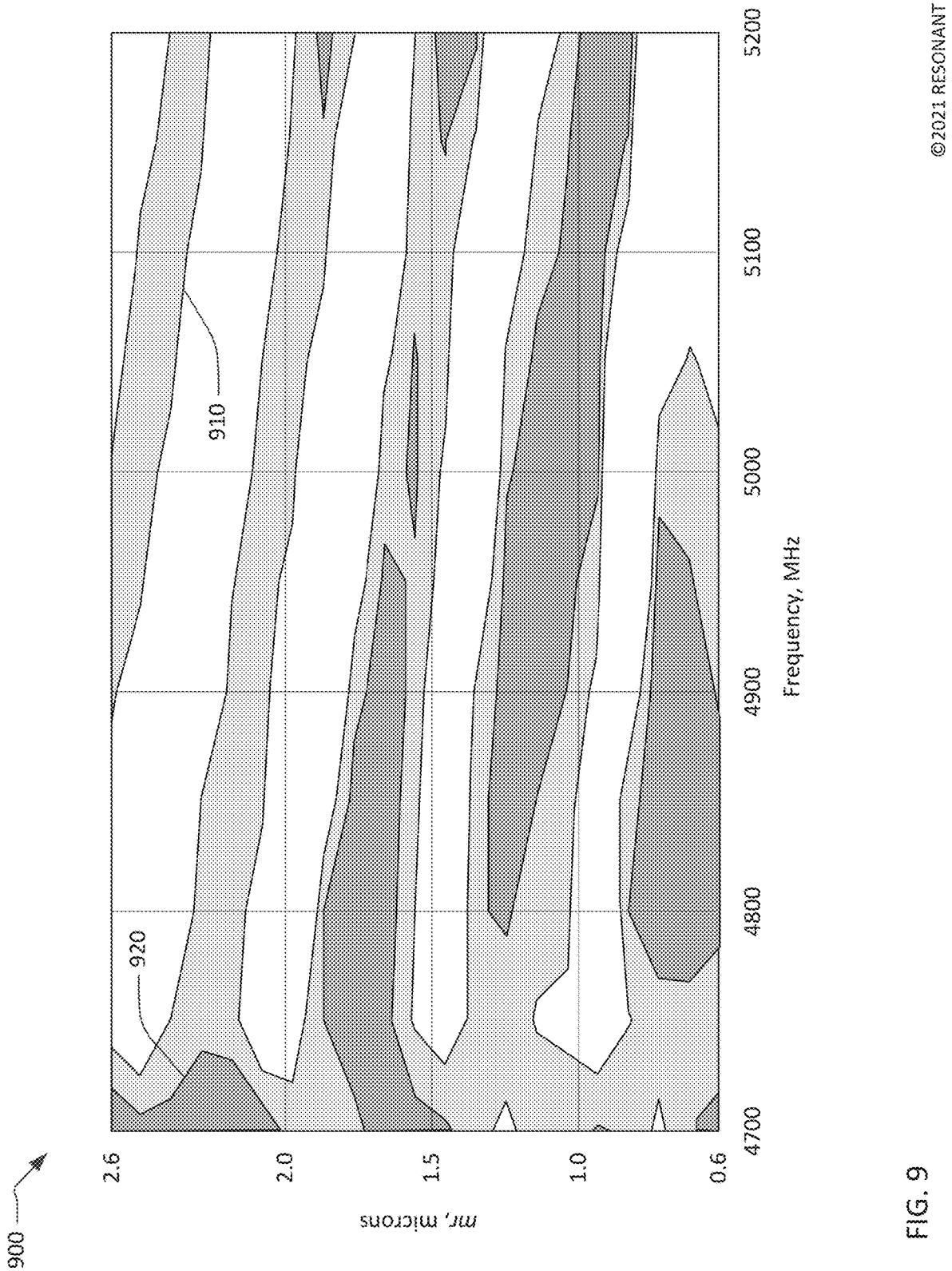
900
2.6
2.0
1.5
1.0
0.6
mr, microns
4700
4800
4900
5000
5100
5200
Frequency, MHz
910
920
©2021 RESONANT INC

FIG. 9

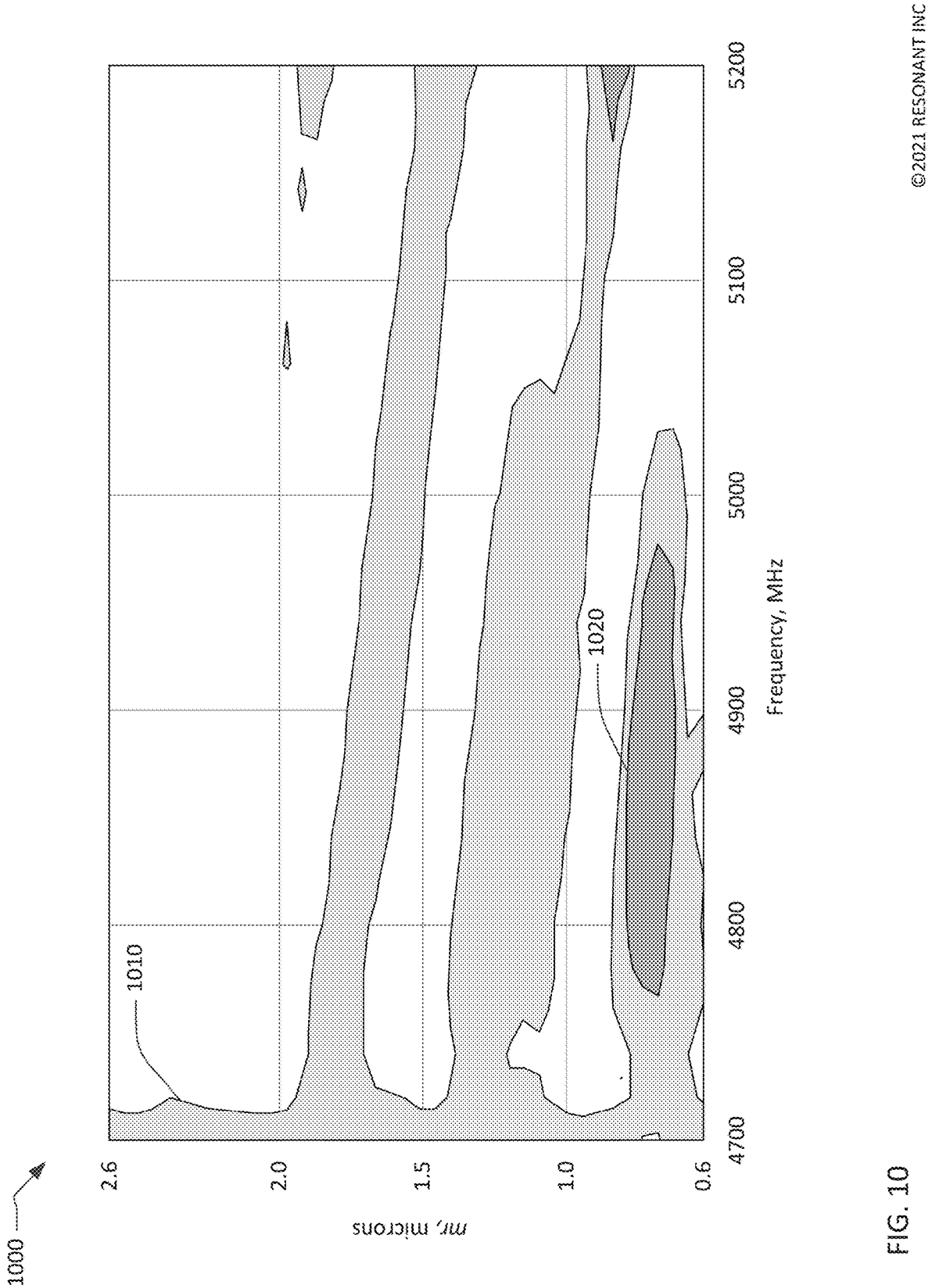
1000
2.6
2.0
1.5
1.0
0.6
nr, microns
4700
4800
4900
5000
5100
5200
Frequency, MHz
1010
1020
©2021 RESONANT INC

FIG. 10

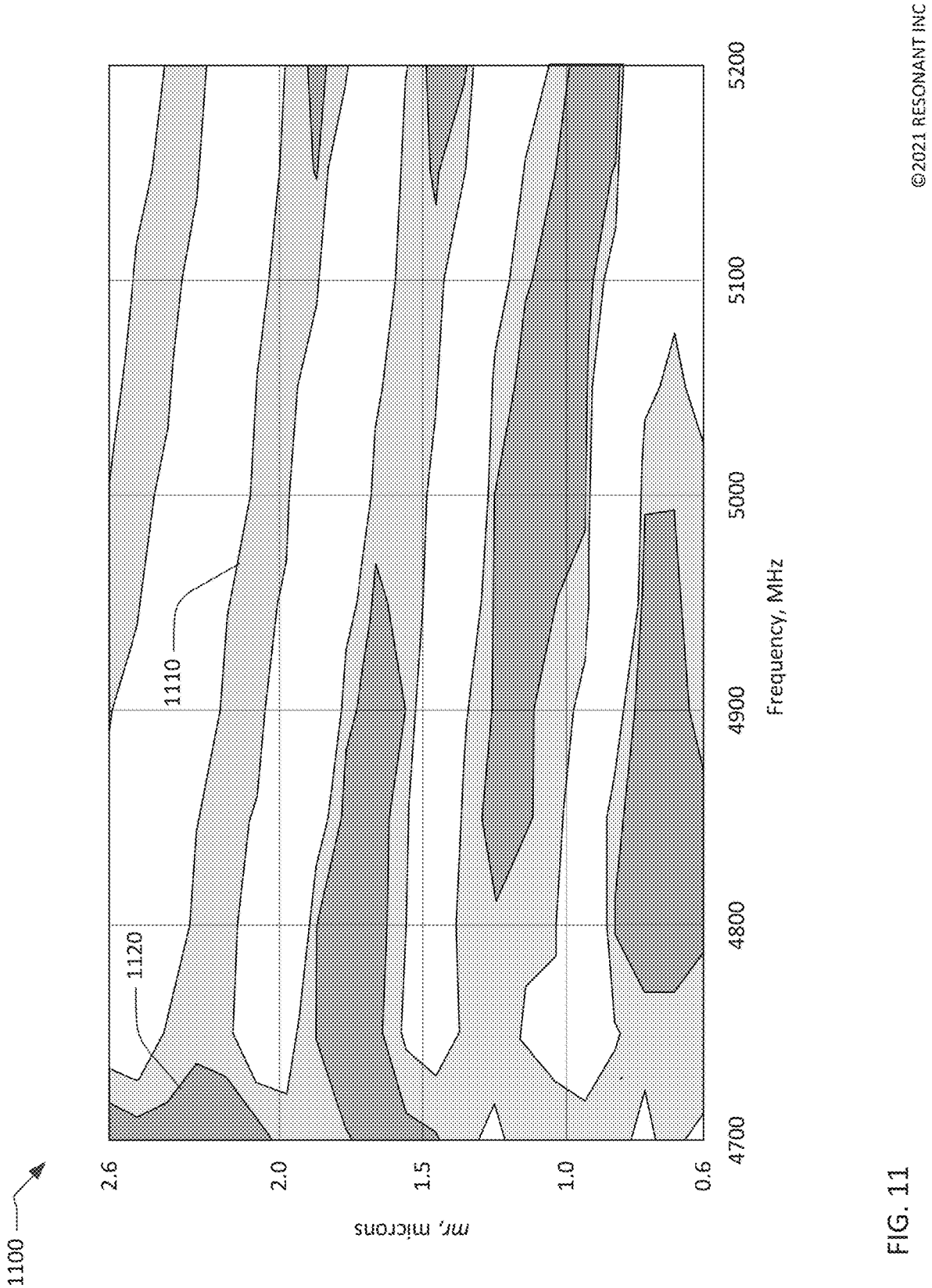
1100
1110
1120
2.6
2.0
1.5
1.0
0.6
mr, microns
4700
4800
4900
5000
5100
5200
Frequency, MHz
©2021 RESONANT INC

FIG. 11

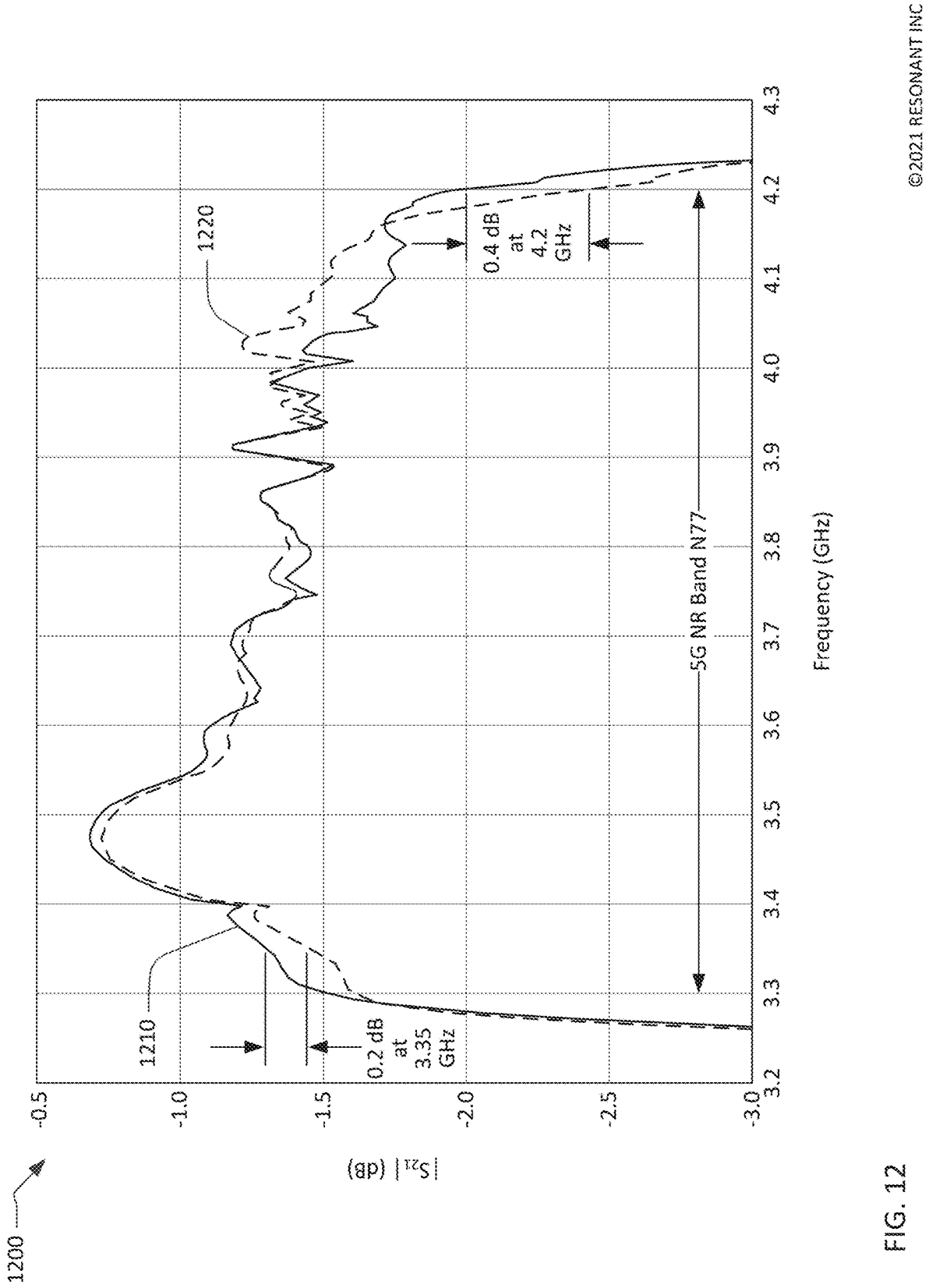
1200
|S21| (dB)
-0.5
-1.0
-1.5
-2.0
-2.5
-3.0
3.2
3.3
3.4
3.5
3.6
3.7
3.8
3.9
4.0
4.1
4.2
4.3
Frequency (GHz)
1210
1220
0.2 dB at 3.35 GHz
0.4 dB at 4.2 GHz
5G NR Band N77
©2021 RESONANT INC

FIG. 12

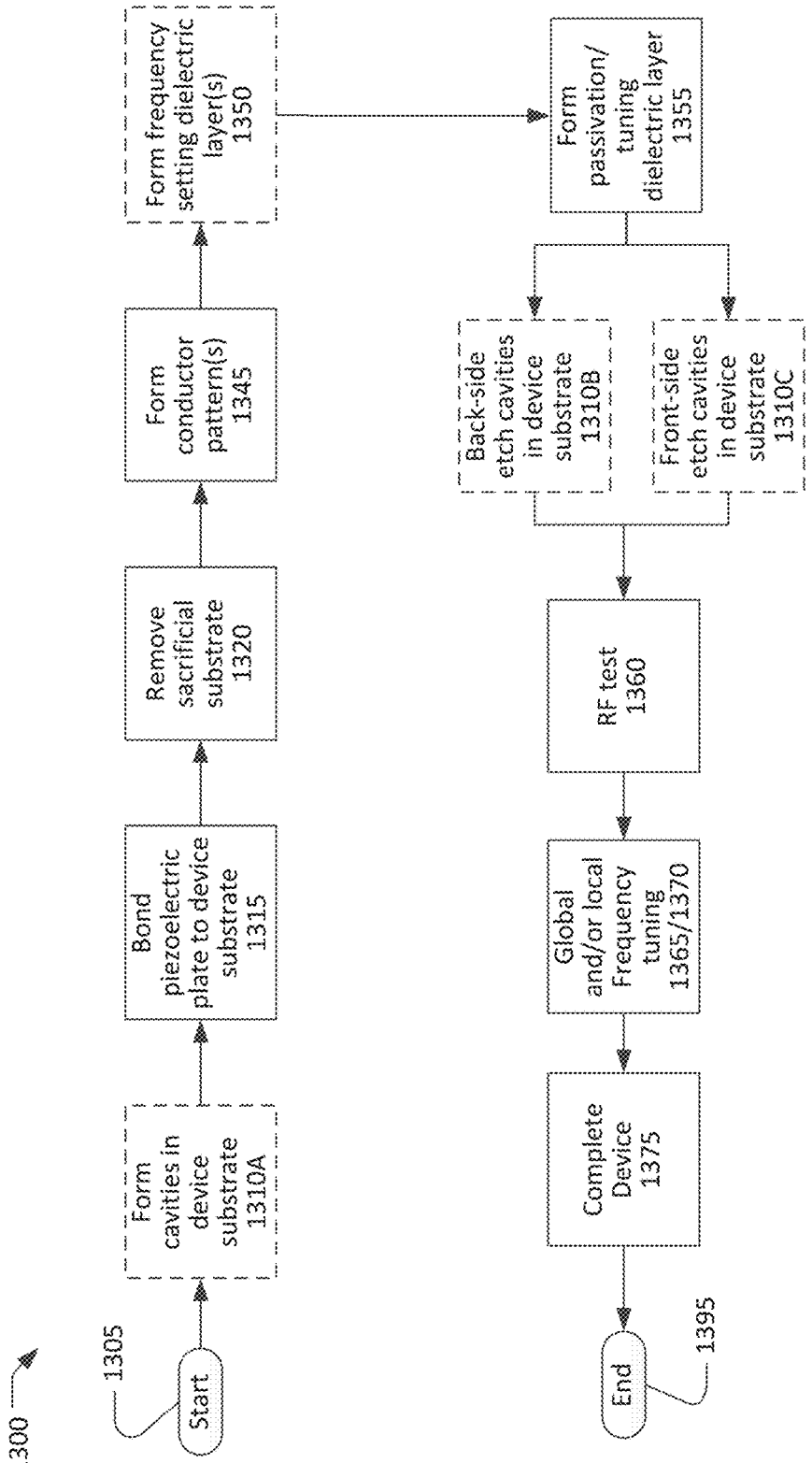

Notes: Only one of actions 1310A, 1310B, 1310C is performed in each of three variations of the process 1300.

FIG. 13

SMALL TRANSVERSELY-EXCITED FILM BULK ACOUSTIC RESONATORS WITH ENHANCED Q-FACTOR

RELATED APPLICATION INFORMATION

This patent is a continuation of application Ser. No. 17/229,767, filed Apr. 13, 2021, entitled SMALL TRANSVERSELY-EXCITED FILM BULK ACOUSTIC RESONATORS WITH ENHANCED Q-FACTOR, which claims priority to the following provisional patent applications: application No. 63/012,849, filed Apr. 20, 2020, entitled SMALL HIGH Q XBAR RESONATORS; application No. 63/066,520, filed Aug. 17, 2020, entitled SMALL REFLECTORS TO IMPROVE XBAR LOSS; and application No. 63/074,991, filed Sep. 4, 2020, entitled SMALL REFLECTORS TO IMPROVE PERFORMANCE OF TRANSVERSELY-EXCITED FILM BUILK ACOUSTIC RESONATORS AT A SPECIFIED FREQUENCY. All of these applications are incorporated herein by reference.

NOTICE OF COPYRIGHTS AND TRADE DRESS

BACKGROUND

Field

This disclosure relates to radio frequency filters using acoustic wave resonators, and specifically to filters for use in communications equipment.

Description of the Related Art

A radio frequency (RF) filter is a two-port device configured to pass some frequencies and to stop other frequencies, where "pass" means transmit with relatively low signal loss and "stop" means block or substantially attenuate. The range of frequencies passed by a filter is referred to as the "pass-band" of the filter. The range of frequencies stopped by such a filter is referred to as the "stop-band" of the filter. A typical RF filter has at least one pass-band and at least one stop-band. Specific requirements on a pass-band or stop-band depend on the application. For example, a "pass-band" may be defined as a frequency range where the insertion loss of a filter is better than a defined value such as 1 dB, 2 dB, or 3 dB. A "stop-band" may be defined as a frequency range where the rejection of a filter is greater than a defined value such as 20 dB, 30 dB, 40 dB, or greater depending on application.

RF filters are used in communications systems where information is transmitted over wireless links. For example, RF filters may be found in the RF front-ends of cellular base stations, mobile telephone and computing devices, satellite transceivers and ground stations, IoT (Internet of Things) devices, laptop computers and tablets, fixed point radio links, and other communications systems. RF filters are also used in radar and electronic and information warfare systems.

RF filters typically require many design trade-offs to achieve, for each specific application, the best compromise between performance parameters such as insertion loss, rejection, isolation, power handling, linearity, size and cost. Specific design and manufacturing methods and enhancements can benefit simultaneously one or several of these requirements.

Performance enhancements to the RF filters in a wireless system can have broad impact to system performance. Improvements in RF filters can be leveraged to provide system performance improvements such as larger cell size, longer battery life, higher data rates, greater network capacity, lower cost, enhanced security, higher reliability, etc. These improvements can be realized at many levels of the wireless system both separately and in combination, for example at the RF module, RF transceiver, mobile or fixed sub-system, or network levels.

High performance RF filters for present communication systems commonly incorporate acoustic wave resonators including surface acoustic wave (SAW) resonators, bulk acoustic wave (BAW) resonators, film bulk acoustic wave resonators (FBAR), and other types of acoustic resonators. However, these existing technologies are not well-suited for use at the higher frequencies and bandwidths proposed for future communications networks.

The desire for wider communication channel bandwidths will inevitably lead to the use of higher frequency communications bands. Radio access technology for mobile telephone networks has been standardized by the 3GPP (3^{rd} Generation Partnership Project). Radio access technology for 5^{th} generation (5G) mobile networks is defined in the 5G NR (new radio) standard. The 5G NR standard defines several new communications bands. Two of these new communications bands are n77, which uses the frequency range from 3300 MHz to 4200 MHz, and n79, which uses the frequency range from 4400 MHz to 5000 MHz. Both band n77 and band n79 use time-division duplexing (TDD), such that a communications device operating in band n77 and/or band n79 use the same frequencies for both uplink and downlink transmissions. Bandpass filters for bands n77 and n79 must be capable of handling the transmit power of the communications device. WiFi bands at 5 GHz and 6 GHz also require high frequency and wide bandwidth. The 5G NR standard also defines millimeter wave communication bands with frequencies between 24.25 GHz and 40 GHz.

The Transversely-Excited Film Bulk Acoustic Resonator (XBAR) is an acoustic resonator structure for use in microwave filters. The XBAR is described in patent U.S. Pat. No. 10,491,291, titled TRANSVERSELY EXCITED FILM BULK ACOUSTIC RESONATOR. An XBAR resonator comprises an interdigital transducer (IDT) formed on a thin floating layer, or diaphragm, of a single-crystal piezoelectric material. The IDT includes a first set of parallel fingers, extending from a first busbar and a second set of parallel fingers extending from a second busbar. The first and second sets of parallel fingers are interleaved. A microwave signal applied to the IDT excites a shear primary acoustic wave in the piezoelectric diaphragm. XBAR resonators provide very high electromechanical coupling and high frequency capability. XBAR resonators may be used in a variety of RF filters including band-reject filters, band-pass filters, duplexers, and multiplexers. XBARs are well suited for use in filters for communications bands with frequencies above 3 GHz.

DESCRIPTION OF THE DRAWINGS

FIG. **1** includes a schematic plan view, two schematic cross-sectional views, and a detail view of a transversely-excited film bulk acoustic resonator (XBAR).

FIG. **2** is a schematic block diagram of a band-pass filter using acoustic resonators.

FIG. **3** is a graph of relationships between the Q-factor of an XBAR and the number of fingers in the interdigital transducer (IDT) of the XBAR.

FIG. **4** is a schematic plan view of an IDT with reflector elements.

FIG. **5** is a schematic plan view of another IDT with reflector elements.

FIG. **6** is a graph comparing the normalized Q-factor of an XBAR with and without reflector elements at the resonance frequency.

FIG. **7** is a graph comparing the normalized Q-factor of an XBAR with and without reflector elements at the anti-resonance frequency.

FIG. **8** is a graph showing relative Q-factor as a function of reflector element pitch and mark for a representative XBAR at a frequency of 5150 MHz.

FIG. **9** is a graph showing relative Q-factor as a function of frequency and reflector element mark for an XBAR with two reflector elements at each end.

FIG. **10** is a graph showing relative Q-factor as a function of frequency and reflector element mark for an XBAR with one reflector element at each end.

FIG. **11** is a graph showing relative Q-factor as a function of frequency and reflector element mark for an XBAR with five reflector elements at each end.

FIG. **12** is a graph comparing the performance of two band-pass filters using XBARs with and without reflector elements.

FIG. **13** is a flow chart of a method for fabricating an XBAR or a filter using XBARs.

Throughout this description, elements appearing in figures are assigned three-digit or four-digit reference designators, where the two least significant digits are specific to the element and the one or two most significant digit is the figure number where the element is first introduced. An element that is not described in conjunction with a figure may be presumed to have the same characteristics and function as a previously-described element having the same reference designator.

DETAILED DESCRIPTION

Description of Apparatus

FIG. **1** shows a simplified schematic top view and orthogonal cross-sectional views of an XBAR **100**. XBAR resonators such as the resonator **100** may be used in a variety of RF filters including band-reject filters, band-pass filters, duplexers, and multiplexers.

The XBAR **100** is made up of a thin film conductor pattern formed on a surface of a piezoelectric plate **110** having parallel front and back surfaces **112**, **114**, respectively. The piezoelectric plate is a thin single-crystal layer of a piezoelectric material such as lithium niobate, lithium tantalate, lanthanum gallium silicate, gallium nitride, or aluminum nitride. The piezoelectric plate is cut such that the orientation of the X, Y, and Z crystalline axes with respect to the front and back surfaces is known and consistent. The piezoelectric plate may be Z-cut, which is to say the Z axis is normal to the front and back surfaces **112**, **114**. The piezoelectric plate may be rotated Z-cut or rotated YX-cut. XBARs may be fabricated on piezoelectric plates with other crystallographic orientations.

The back surface **114** of the piezoelectric plate **110** is attached to a surface of a substrate **120** except for a portion of the piezoelectric plate **110** that forms a diaphragm **115** spanning a cavity **140** formed in the substrate. The portion of the piezoelectric plate that spans the cavity is referred to herein as the "diaphragm" **115** due to its physical resemblance to the diaphragm of a microphone. As shown in FIG. **1**, the diaphragm **115** is contiguous with the rest of the piezoelectric plate **110** around all of a perimeter **145** of the cavity **140**. In this context, "contiguous" means "continuously connected without any intervening item". In other configurations, the diaphragm **115** may be contiguous with the piezoelectric plate around at least 50% of the perimeter **145** of the cavity **140**.

The substrate **120** provides mechanical support to the piezoelectric plate **110**. The substrate **120** may be, for example, silicon, sapphire, quartz, or some other material or combination of materials. The back surface **114** of the piezoelectric plate **110** may be bonded to the substrate **120** using a wafer bonding process. Alternatively, the piezoelectric plate **110** may be grown on the substrate **120** or attached to the substrate in some other manner. The piezoelectric plate **110** may be attached directly to the substrate or may be attached to the substrate **120** via one or more intermediate material layers (not shown in FIG. **1**).

"Cavity" has its conventional meaning of "an empty space within a solid body." The cavity **140** may be a hole completely through the substrate **120** (as shown in Section A-A and Section B-B) or a recess in the substrate **120** under the diaphragm **115**. The cavity **140** may be formed, for example, by selective etching of the substrate **120** before or after the piezoelectric plate **110** and the substrate **120** are attached.

The conductor pattern of the XBAR **100** includes an interdigital transducer (IDT) **130**. The IDT **130** includes a first plurality of parallel fingers, such as finger **136**, extending from a first busbar **132** and a second plurality of fingers extending from a second busbar **134**. The term "busbar" means a conductor from which the fingers of an IDT extend. The first and second pluralities of parallel fingers are interleaved. The interleaved fingers overlap for a distance AP, commonly referred to as the "aperture" of the IDT. The center-to-center distance L between the outermost fingers of the IDT **130** is the "length" of the IDT.

The first and second busbars **132**, **134** serve as the terminals of the XBAR **100**. A radio frequency or microwave signal applied between the two busbars **132**, **134** of the IDT **130** excites a primary acoustic mode within the piezoelectric plate **110**. The primary acoustic mode is a bulk shear mode where acoustic energy propagates along a direction substantially orthogonal to the surface of the piezoelectric plate **110**, which is also normal, or transverse, to the direction of the electric field created by the IDT fingers. Thus, the XBAR is considered a transversely-excited film bulk wave resonator.

The IDT **130** is positioned on the piezoelectric plate **110** such that at least the fingers of the IDT **130** are disposed on the diaphragm **115** that spans, or is suspended over, the cavity **140**. As shown in FIG. **1**, the cavity **140** has a rectangular shape with an extent greater than the aperture AP and length L of the IDT **130**. A cavity of an XBAR may have a different shape, such as a regular or irregular polygon. The cavity of an XBAR may more or fewer than four sides, which may be straight or curved.

For ease of presentation in FIG. **1**, the geometric pitch and width of the IDT fingers are greatly exaggerated with respect to the length (dimension L) and aperture (dimension AP) of the XBAR. A typical XBAR has more than ten parallel fingers in the IDT **130**. An XBAR may have hundreds, possibly thousands, of parallel fingers in the IDT **130**. Similarly, the thicknesses of the IDT fingers and the piezoelectric plate in the cross-sectional views are greatly exaggerated.

Referring now to the detailed schematic cross-sectional view, a front-side dielectric layer **150** may optionally be formed on the front side of the piezoelectric plate **110**. The "front side" of the XBAR is, by definition, the surface facing away from the substrate. The front-side dielectric layer **150** may be formed only between the IDT fingers (e.g. IDT finger **138***b*) or may be deposited as a blanket layer such that the dielectric layer is formed both between and over the IDT fingers (e.g. IDT finger **138***a*). The front-side dielectric layer **150** may be a non-piezoelectric dielectric material, such as silicon dioxide, alumina, or silicon nitride. A thickness of the front side dielectric layer **150** is typically less than about one-third of the thickness tp of the piezoelectric plate **110**. The front-side dielectric layer **150** may be formed of multiple layers of two or more materials. In some applications, a back-side dielectric layer (not shown) may be formed on the back side of the piezoelectric plate **110**.

The IDT fingers **138***a*, **138***b* may be one or more layers of aluminum, an aluminum alloy, copper, a copper alloy, beryllium, gold, tungsten, molybdenum, chromium, titanium or some other conductive material. The IDT fingers are considered to be "substantially aluminum" if they are formed from aluminum or an alloy comprising at least 50% aluminum. The IDT fingers are considered to be "substantially copper" if they are formed from copper or an alloy comprising at least 50% copper. Thin (relative to the total thickness of the conductors) layers of metals such as chromium or titanium may be formed under and/or over and/or as layers within the fingers to improve adhesion between the fingers and the piezoelectric plate **110** and/or to passivate or encapsulate the fingers and/or to improve power handling. The busbars (**132**, **134** in FIG. **1**) of the IDT may be made of the same or different materials as the fingers.

Dimension p is the center-to-center spacing or "pitch" of the IDT fingers, which may be referred to as the pitch of the IDT and/or the pitch of the XBAR. Dimension m is the width or "mark" of the IDT fingers. The geometry of the IDT of an XBAR differs substantially from the IDTs used in surface acoustic wave (SAW) resonators. In a SAW resonator, the pitch of the IDT is one-half of the acoustic wavelength at the resonance frequency. Additionally, the mark-to-pitch ratio of a SAW resonator IDT is typically close to 0.5 (i.e. the mark or finger width is about one-fourth of the acoustic wavelength at resonance). In an XBAR, the pitch p of the IDT may be 2 to 20 times the width m of the fingers. The pitch p is typically 3.3 to 5 times the width m of the fingers. In addition, the pitch p of the IDT may be 2 to 20 times the thickness of the piezoelectric plate **210**. The pitch p of the IDT is typically 5 to 12.5 times the thickness of the piezoelectric plate **210**. The width m of the IDT fingers in an XBAR is not constrained to be near one-fourth of the acoustic wavelength at resonance. For example, the width of XBAR IDT fingers may be 500 nm or greater, such that the IDT can be readily fabricated using optical lithography. The thickness of the IDT fingers may be from 100 nm to about equal to the width m. The thickness of the busbars (**132**, **134**) of the IDT may be the same as, or greater than, the thickness tm of the IDT fingers.

FIG. **2** is a schematic circuit diagram and layout for a high frequency band-pass filter **200** using XBARs. The filter **200** has a conventional ladder filter architecture including three series resonators **210**A, **210**B, **210**C and two shunt resonators **220**A, **220**B. The three series resonators **210**A, **210**B, and **210**C are connected in series between a first port and a second port (hence the term "series resonator"). In FIG. **2**, the first and second ports are labeled "In" and "Out", respectively. However, the filter **200** is bidirectional and either port may serve as the input or output of the filter. The two shunt resonators **220**A, **220**B are connected from nodes between the series resonators to ground. A filter may contain additional reactive components, such as capacitors and/or inductors, not shown in FIG. **2**. All the shunt resonators and series resonators are XBARs. The inclusion of three series and two shunt resonators is exemplary. A filter may have more or fewer than five total resonators, more or fewer than three series resonators, and more or fewer than two shunt resonators. Typically, all of the series resonators are connected in series between an input and an output of the filter. All of the shunt resonators are typically connected between ground and the input, the output, or a node between two series resonators.

In the exemplary filter **200**, the three series resonators **210**A, B, C and the two shunt resonators **220**A, B of the filter **200** are formed on a single plate **230** of piezoelectric material bonded to a silicon substrate (not visible). In some filters, the series resonators and shunt resonators may be formed on different plates of piezoelectric material. Each resonator includes a respective IDT (not shown), with at least the fingers of the IDT disposed over a cavity in the substrate. In this and similar contexts, the term "respective" means "relating things each to each", which is to say with a one-to-one correspondence. In FIG. **2**, the cavities are illustrated schematically as the dashed rectangles (such as the rectangle **235**). In this example, each IDT is disposed over a respective cavity. In other filters, the IDTs of two or more resonators may be disposed over a single cavity.

Each of the resonators **210**A, **210**B, **210**C, **220**A, **220**B in the filter **200** has resonance where the admittance of the resonator is very high and an anti-resonance where the admittance of the resonator is very low. The resonance and anti-resonance occur at a resonance frequency and an anti-resonance frequency, respectively, which may be the same or different for the various resonators in the filter **200**. In over-simplified terms, each resonator can be considered a short-circuit at its resonance frequency and an open circuit at its anti-resonance frequency. The input-output transfer function will be near zero at the resonance frequencies of the shunt resonators and at the anti-resonance frequencies of the series resonators. In a typical filter, the resonance frequencies of the shunt resonators are positioned below the lower edge of the filter's passband and the anti-resonance frequencies of the series resonators are positioned above the upper edge of the passband. In some filters, a front-side dielectric layer (also called a "frequency setting layer"), represented by the dot-dash rectangle **270**, may be formed on the shunt resonators to set the resonance frequencies of the shunt resonators lower relative to the resonance frequencies of the series resonators.

The Q-factor of an acoustic resonator is commonly defined as the peak energy stored during a cycle of the applied RF signal divided by the total energy dissipated or lost during the cycle. The Q-factor of an XBAR is a complex function of numerous parameters including the length, or number of fingers, in the IDT of the XBAR.

Possible loss mechanisms in an acoustic resonator include resistive losses in the IDT and other conductors; viscous or acoustic losses in the piezoelectric plate, IDT fingers, and other materials; and leakage of acoustic energy out of the resonator structure. The peak energy stored in a resonator is proportional the capacitance of the resonator. In an XBAR resonator, the capacitance is proportional to the number of IDT fingers. Resistive losses and viscous losses are also proportional to the number of IDT fingers. Acoustic energy that leaks from the resonator in the transverse direction (i.e. the direction parallel to the IDT fingers) is proportional to the length of the resonator and thus also proportional to the number of IDT fingers. In contrast, energy lost from the ends of the IDT in the longitudinal direction (i.e. the direction normal to the IDT fingers) is roughly constant, independent of the number of IDT fingers. As the number of IDT fingers and the peak energy stored in an XBAR is reduced, the acoustic energy lost in the longitudinal direction becomes an ever-increasing fraction of the peak energy stored.

FIG. **3** is a graph of the normalized Q factor of a representative XBAR as a function of the number of fingers in the IDT of the XBAR. The "normalized Q-factor" is the Q-factor of the XBAR with a finite number of IDT fingers divided by the Q-factor of a hypothetical XBAR with the same structure and an infinite number of IDT fingers. In FIG. **3**, normalized Q-factor is quantified as a percentage of the Q-factor of the XBAR with an infinite number of IDT fingers. Specifically, the solid curve **310** is a plot of the normalized Q-factor at the resonance frequency and the dashed curve **320** is a plot of the normalized Q-factor at the anti-resonance frequency. The data in FIG. **3** is derived from simulations using a finite element method.

FIG. **3** shows that the normalized Q-factor of an XBAR with a finite number of IDT fingers is less than 100%, which is to say the Q-factor of an XBAR with a finite number of IDT fingers is less than the Q-factor of a similar XBAR with an infinite number of IDT fingers. Although not shown in FIG. **3**, the normalized Q-factor of an XBAR may asymptotically approach 100% for a very large number of IDT fingers. As anticipated, the normalized Q-factor depends on the number of IDT fingers. In particular, the normalized Q-factor decreases precipitously for XBARs with less than about 20 IDT fingers due to the increasing significance of acoustic energy lost in the longitudinal direction.

FIG. **4** is a plan view of an exemplary conductor pattern **400** that reduces the acoustic energy leakage in the longitudinal direction at the ends of an XBAR. The conductor pattern **400** includes an IDT **430** and four reflector elements **462**, **464**, **466**, **468**. The IDT **430** includes a first busbar **432**, a second busbar **434**, and a plurality of n interleaved IDT fingers extending alternately from the first and second busbars. In this example, n, the number of IDT fingers, is equal to 24. In other XBARs, n may be in a range from 20 to 100 or more IDT fingers. IDT finger **436** is the 1st finger and IDT finger **438** is the n'th finger. Numbering the IDT fingers from left to right (as shown in FIG. **4**) is arbitrary and the designations of the 1st and n'th fingers could be reversed.

As shown in FIG. **4**, the odd numbered IDT fingers extend from the first busbar **432** and the even numbered IDT fingers extend from the second busbar **434**. The IDT **430** has an even number of IDT fingers such that the 1st and n'th IDT fingers **436**, **438** extend from different busbars. In some cases, an IDT may have an odd number of IDT fingers such that the 1st and n'th IDT fingers and all of the reflector elements extend from the same busbar.

A total of four reflector elements are provided outside of periphery of the IDT **430**. A first reflector element **462** is proximate and parallel to 1st IDT finger **436** at the left end of the IDT **430**. A second reflector element **466** is proximate and parallel to n'th IDT finger **438** at the right end of the IDT **430**. An optional third reflector element **464** is parallel to the first reflector element **462**. An optional fourth reflector element **468** is parallel to the second reflector element **466**.

First and third reflector elements **462**, **464** extend from the first busbar **432** and thus are at the same electrical potential as the 1st IDT finger **436**. Similarly, second and fourth reflector elements **466** and **468** extend from the second busbar **430** and thus are at the same electrical potential as the n'th IDT finger **438**.

The reflector elements **462**, **464**, **466**, **468** are configured to confine acoustic energy to the area of the IDT **430** and thus reduce acoustic energy losses in the longitudinal direction. To this end, the pitch pr between adjacent reflector elements and between reflector elements **462** and **466** and the adjacent first and n'th IDT fingers, respectively, is typically greater than the pitch p of the IDT fingers. The width or mark mr of the reflector elements **462**, **464**, **466**, **468** is not necessarily equal to the mark m of the IDT fingers. As will be described subsequently, the mark mr of the reflector elements may be selected to optimize Q-factor at a specific frequency or range of frequencies.

FIG. **5** is a plan view of another conductor pattern **500** that reduces the acoustic energy leakage in the longitudinal direction at the ends of an XBAR. The conductor pattern **500** includes an IDT **530** and four reflector elements **562**, **564**, **566**, **568**. The IDT **530** includes a first busbar **532**, a second busbar **534**, and a plurality of interleaved IDT fingers extending alternately from the first and second busbars as previously described. IDT fingers **536** and **538** are the 1st and n'th IDT fingers at the left and right (as shown in FIG. **5**) ends of the IDT **530**.

A total of four reflector elements are provided outside of periphery of the IDT **530**. First and third reflector elements **562** and **564** are proximate and parallel to 1st IDT finger **536** at the left end of the IDT **530**. First and third reflector elements **562**, **564** are connected to each other but are not connected to either busbar **532**, **534**. First and third reflector elements **562**, **564** are capacitively coupled to 1st IDT finger **536** and thus are at substantially the same electrical potential as the 1st IDT finger **536**. The reflector elements are considered to be at substantially the same potential if, when an RF signal is applied between the busbars **532**, **534**, the potential between the reflector elements and the 1st IDT finger is small compared to the potential between adjacent IDT fingers.

Similarly, second and fourth reflector elements **566** and **568** are proximate and parallel to n'th IDT finger **538** at the right end of the IDT **530**. Second and fourth reflector elements **566**, **568** are connected to each other and not connected to either busbar **532**, **534**. Second and fourth reflector elements **566**, **568** are capacitively coupled to the n'th IDT finger **538** and thus are at nearly the same electrical potential as the n'th IDT finger **538**.

The reflector elements **562**, **564**, **566**, **568** are configured to confine acoustic energy to the area of the IDT **530** and thus reduce acoustic energy lost in the longitudinal direction. To this end, the pitch pr between adjacent reflector elements and between reflector elements **562** and **566** and the adjacent terminal IDT fingers is typically greater than the pitch p of the IDT fingers. The width or mark mr of the reflector elements **562**, **564**, **566**, **568** is not necessarily equal to the mark m of the IDT fingers. The mark mr of the reflector elements may be selected to optimize Q-factor for a particular frequency of range of frequencies.

FIG. **6** is a graph of the normalized Q-factor as a function of number of IDT fingers for another XBAR with and without reflector elements similar to the reflector elements shown in FIG. **4**. Specifically, the solid curve **610** is a plot of the normalized Q-factor of an XBAR without reflector elements at its resonance frequency. The dashed curve **620** is a plot of the normalized Q-factor at the resonance frequency for a similar XBAR with two reflector elements at each side of the IDT. In both cases, the piezoelectric plate is lithium niobate 400 nm thick, the IDT fingers are aluminum 500 nm thick, IDT pitch p=4 microns, and IDT finger mark m=1 micron. For the XBAR with reflector elements, pr=4.2 microns and mr=0.735 microns. With reflector elements, an XBAR with as few as 10 fingers can have a normalized Q-factor up to 80%.

FIG. **7** is a graph of the normalized Q-factor as a function of number of IDT fingers for another XBAR with and without reflector elements similar to the reflector elements shown in FIG. **4**. Specifically, the solid curve **710** is a plot of the normalized Q-factor of an XBAR without reflector elements at its anti-resonance frequency. The dashed curve **720** is a plot of the normalized Q-factor at the anti-resonance frequency for a similar XBAR with two reflector elements at each side of the IDT. In both cases, the piezoelectric plate is lithium niobate 400 nm thick, the IDT fingers are aluminum 500 nm thick, IDT pitch p=4 microns, and IDT finger mark m=1 micron. For the XBAR with reflector elements, pr=8 microns and mr=0.80 microns. With reflector elements, an XBAR with as few as 14 fingers can have a normalized Q-factor up to 80%.

FIG. **8** shows a chart **800** illustrating the relationship between the pitch pr and mark mr of reflector elements of an exemplary XBAR device at a fixed frequency of 5150 MHz. The exemplary XBAR device has a lithium niobate piezoelectric plate with a thickness of 400 nm and aluminum IDT and reflector elements with a thickness of 500 nm. The pitch and mark of the IDT fingers are 4 microns and 1 micron, respectively. There are two reflector elements at each end of the IDT. The lighter shaded area **810**A, **810**B, **810**C, **810**D identify combinations of pr and mr where the normalized Q-factor is greater than or equal to 85%. The darker shaded area **820**A, **820**B, **820**C, **820**D identify combinations of pr and mr where the normalized Q-factor is greater than or equal to 90%. For comparison, the normalized Q-factor of this XBAR without reflector elements is 74% at 5150 MHz. Although not identified in FIG. **8** there are combinations of pr and mr where the normalized Q-factor is less than 75%, indicating improperly configured reflector elements can degrade XBAR Q-factor.

There are multiple combinations of pr and mr that raise the normalized Q-factor to 85% or 90%. To achieve a normalized Q-factor of greater than or equal to 90%, pr must be greater than or equal to 1.2 times the pitch p of the IDT fingers. For pr=6 microns (1.5p), there are at least four values of mr that raise the normalized Q-factor to more than 90%.

FIG. **9** shows a chart **900** illustrating the relationship between the mark mr of reflector elements and frequency for an exemplary XBAR device with two reflector elements at each side of an IDT and pr=5.2 microns. As in the previous examples, the exemplary XBAR device has a lithium niobate piezoelectric plate with a thickness of 400 nm and aluminum IDT and reflector elements with a thickness of 500 nm. The pitch and mark of the IDT fingers are 4 microns and 1 micron, respectively. Lighter shaded areas such as area **910** identify combinations of frequency and mr where the normalized Q-factor is greater than or equal to 85%. Darker shaded areas such as area **920** identify combinations of frequency and mr where the normalized Q-factor is greater than or equal to 90%. For comparison, the normalized Q-factor of this XBAR without reflector elements is 74% at 5150 MHz.

The chart **900** illustrates that, for a particular reflector element pitch pr, reflector element mark mr must be selected with consideration of the frequency where the Q-factor of an XBAR needs improvement. For example, selecting mr=0.95 microns provides a normalized Q-factor greater than 90% over a frequency range from about 4980 MHz to greater than 5200 MHz. Selecting mr=1.7 microns provides a normalized Q-factor greater than 90% over a frequency range of less than 4700 MHz to about 4950 MHz. However, selecting mr=1.7 microns may actually lower the Q-factor at 5200 MHz compared to an XBAR with no reflector elements.

FIG. **10** shows a chart **11000** illustrating the relationship between the mark mr of reflector elements and frequency for an exemplary XBAR device with one reflector element at each side of an IDT and pr=5.2 microns. The exemplary XBAR device is the same as the previous examples. As in FIG. **9**, lighter shaded areas such as area **1010** identify combinations of frequency and mr where the normalized Q-factor is greater than or equal to 85%. Darker shaded areas such as area **1020** identify combinations of frequency and mr where the normalized Q-factor is greater than or equal to 90%.

Comparison of FIG. **9** and FIG. **10** shows that a only one reflector element is generally less effective that two reflector elements for at improving normalized Q-factor. However, in some applications one reflector element at each end of an IDT may be sufficient. In this example, one reflector element (at each end of the IDT) with mr=0.75 microns provides a substantial improvement in normalized Q-factor for a frequency range of about 4770 MHz to 4970 MHz.

FIG. **11** shows a chart **1100** illustrating the relationship between the mark mr of reflector elements and frequency for an exemplary XBAR device with five reflector elements at each end of an IDT and pr=5.2 microns. The exemplary XBAR device is the same as the previous examples. As in FIG. **9**, lighter shaded areas such as area **1110** identify combinations of frequency and mr where the normalized Q-factor is greater than or equal to 85%. Darker shaded areas such as area **1120** identify combinations of frequency and mr where the normalized Q-factor is greater than or equal to 90%.

Comparison of FIG. **9** and FIG. **11** shows that five reflector elements do not provide any significant improvement over two reflector elements.

FIG. **12** is a chart of the performance of an exemplary XBAR bandpass filter with and without reflector elements. Specifically, the solid line **1210** is a plot of the magnitude of S_{21} (the input-output transfer function) of a Band N77 filter with two reflector elements at each end of the XBARs in the filter. The reflector elements of shunt resonators were optimized for a frequency of 3.35 GHz and the reflector elements of series resonators were optimized for a frequency of 4.2 GHz. These frequencies are at or near the edges of the N77 band where it is typically most difficult to achieve requirements on minimum S_{21}. The dashed line **1220** is a plot of the magnitude of S_{21} for the same filter without reflector elements on the XBARs. All of the data was developed by simulations of the filters using a finite element method.

The inclusion of reflector elements improves S_{21} by 0.2 db at 3.35 GHz and by 0.4 dB at 4.2 GHz. Note, however, that the inclusion of the reflector elements reduces S_{21} by as

much as 0.25 dB at other frequencies, illustrating a tradeoff to be made during the design of an XBAR filter. In the exemplary bandpass filter of FIG. **12**, the reflector elements for all of the shunt resonators were selected for maximum Q-factor at the same frequency (3.35 GHz) and the reflector elements for all of the series resonators were selected for maximum Q-factor at the same frequency (4.2 GHz). Further improvements in the filter transfer function are likely if the reflector elements for each resonator are optimized independently.

Description of Methods

FIG. **13** is a simplified flow chart summarizing a process **1300** for fabricating a filter device incorporating XBARs. Specifically, the process **1300** is for fabricating a filter device including multiple XBARs, some of which may include a frequency setting dielectric layer. The process **1300** starts at **1305** with a device substrate and a thin plate of piezoelectric material disposed on a sacrificial substrate. The process **1300** ends at **1395** with a completed filter device. The flow chart of FIG. **13** includes only major process steps. Various conventional process steps (e.g. surface preparation, cleaning, inspection, baking, annealing, monitoring, testing, etc.) may be performed before, between, after, and during the steps shown in FIG. **13**.

While FIG. **13** generally describes a process for fabricating a single filter device, multiple filter devices may be fabricated simultaneously on a common wafer (consisting of a piezoelectric plate bonded to a substrate). In this case, each step of the process **1300** may be performed concurrently on all of the filter devices on the wafer.

The flow chart of FIG. **13** captures three variations of the process **1300** for making an XBAR which differ in when and how cavities are formed in the device substrate. The cavities may be formed at steps **1310**A, **1310**B, or **1310**C. Only one of these steps is performed in each of the three variations of the process **1300**.

The piezoelectric plate may be, for example, lithium niobate or lithium tantalate, either of which may be Z-cut, rotated Z-cut, or rotated YX-cut. The piezoelectric plate may be some other material and/or some other cut. The device substrate may preferably be silicon. The device substrate may be some other material that allows formation of deep cavities by etching or other processing.

In one variation of the process **1300**, one or more cavities are formed in the device substrate at **1310**A, before the piezoelectric plate is bonded to the substrate at **1315**. A separate cavity may be formed for each resonator in a filter device. The one or more cavities may be formed using conventional photolithographic and etching techniques. Typically, the cavities formed at **1310**A will not penetrate through the device substrate.

At **1315**, the piezoelectric plate is bonded to the device substrate. The piezoelectric plate and the device substrate may be bonded by a wafer bonding process. Typically, the mating surfaces of the device substrate and the piezoelectric plate are highly polished. One or more layers of intermediate materials, such as an oxide or metal, may be formed or deposited on the mating surface of one or both of the piezoelectric plate and the device substrate. One or both mating surfaces may be activated using, for example, a plasma process. The mating surfaces may then be pressed together with considerable force to establish molecular bonds between the piezoelectric plate and the device substrate or intermediate material layers.

At **1320**, the sacrificial substrate may be removed. For example, the piezoelectric plate and the sacrificial substrate may be a wafer of piezoelectric material that has been ion implanted to create defects in the crystal structure along a plane that defines a boundary between what will become the piezoelectric plate and the sacrificial substrate. At **1320**, the wafer may be split along the defect plane, for example by thermal shock, detaching the sacrificial substrate and leaving the piezoelectric plate bonded to the device substrate. The exposed surface of the piezoelectric plate may be polished or processed in some manner after the sacrificial substrate is detached.

Thin plates of single-crystal piezoelectric materials laminated to a non-piezoelectric substrate are commercially available. At the time of this application, both lithium niobate and lithium tantalate plates are available bonded to various substrates including silicon, quartz, and fused silica. Thin plates of other piezoelectric materials may be available now or in the future. The thickness of the piezoelectric plate may be between 300 nm and 1000 nm. When the substrate is silicon, a layer of SiO_2 may be disposed between the piezoelectric plate and the substrate. When a commercially available piezoelectric plate/device substrate laminate is used, steps **1310**A, **1315**, and **1320** of the process **1300** are not performed.

A first conductor pattern, including IDTs and reflector elements of each XBAR, is formed at **1345** by depositing and patterning one or more conductor layers on the front side of the piezoelectric plate. The conductor layer may be, for example, aluminum, an aluminum alloy, copper, a copper alloy, or some other conductive metal. Optionally, one or more layers of other materials may be disposed below (i.e. between the conductor layer and the piezoelectric plate) and/or on top of the conductor layer. For example, a thin film of titanium, chrome, or other metal may be used to improve the adhesion between the conductor layer and the piezoelectric plate. A second conductor pattern of gold, aluminum, copper or other higher conductivity metal may be formed over portions of the first conductor pattern (for example the IDT bus bars and interconnections between the IDTs).

Each conductor pattern may be formed at **1345** by depositing the conductor layer and, optionally, one or more other metal layers in sequence over the surface of the piezoelectric plate. The excess metal may then be removed by etching through patterned photoresist. The conductor layer can be etched, for example, by plasma etching, reactive ion etching, wet chemical etching, or other etching techniques.

Alternatively, each conductor pattern may be formed at **1345** using a lift-off process. Photoresist may be deposited over the piezoelectric plate. and patterned to define the conductor pattern. The conductor layer and, optionally, one or more other layers may be deposited in sequence over the surface of the piezoelectric plate. The photoresist may then be removed, which removes the excess material, leaving the conductor pattern.

At **1350**, one or more frequency setting dielectric layer(s) may be formed by depositing one or more layers of dielectric material on the front side of the piezoelectric plate. For example, a dielectric layer may be formed over the shunt resonators to lower the frequencies of the shunt resonators relative to the frequencies of the series resonators. The one or more dielectric layers may be deposited using a conventional deposition technique such as physical vapor deposition, atomic layer deposition, chemical vapor deposition, or some other method. One or more lithography processes (using photomasks) may be used to limit the deposition of the dielectric layers to selected areas of the piezoelectric

plate. For example, a mask may be used to limit a dielectric layer to cover only the shunt resonators.

At **1355**, a passivation/tuning dielectric layer is deposited over the piezoelectric plate and conductor patterns. The passivation/tuning dielectric layer may cover the entire surface of the filter except for pads for electrical connections to circuitry external to the filter. In some instantiations of the process **1300**, the passivation/tuning dielectric layer may be formed after the cavities in the device substrate are etched at either **1310**B or **1310**C.

In a second variation of the process **1300**, one or more cavities are formed in the back side of the device substrate at **1310**B. A separate cavity may be formed for each resonator in a filter device. The one or more cavities may be formed using an anisotropic or orientation-dependent dry or wet etch to open holes through the back side of the device substrate to the piezoelectric plate. In this case, the resulting resonator devices will have a cross-section as shown in FIG. **1**.

In a third variation of the process **1300**, one or more cavities in the form of recesses in the device substrate may be formed at **1310**C by etching the substrate using an etchant introduced through openings in the piezoelectric plate. A separate cavity may be formed for each resonator in a filter device. The one or more cavities formed at **1310**C will not penetrate through the device substrate.

Ideally, after the cavities are formed at **1310**B or **1310**C, most or all of the filter devices on a wafer will meet a set of performance requirements. However, normal process tolerances will result in variations in parameters such as the thicknesses of dielectric layer formed at **1350** and **1355**, variations in the thickness and line widths of conductors and IDT fingers formed at **1345**, and variations in the thickness of the piezoelectric plate. These variations contribute to deviations of the filter device performance from the set of performance requirements.

To improve the yield of filter devices meeting the performance requirements, frequency tuning may be performed by selectively adjusting the thickness of the passivation/tuning layer deposited over the resonators at **1355**. The frequency of a filter device passband can be lowered by adding material to the passivation/tuning layer, and the frequency of the filter device passband can be increased by removing material to the passivation/tuning layer. Typically, the process **1300** is biased to produce filter devices with passbands that are initially lower than a required frequency range but can be tuned to the desired frequency range by removing material from the surface of the passivation/tuning layer.

At **1360**, a probe card or other means may be used to make electrical connections with the filter to allow radio frequency (RF) tests and measurements of filter characteristics such as input-output transfer function. Typically, RF measurements are made on all, or a large portion, of the filter devices fabricated simultaneously on a common piezoelectric plate and substrate.

At **1365**, global frequency tuning may be performed by removing material from the surface of the passivation/tuning layer using a selective material removal tool such as, for example, a scanning ion mill as previously described. "Global" tuning is performed with a spatial resolution equal to or larger than an individual filter device. The objective of global tuning is to move the passband of each filter device towards a desired frequency range. The test results from **1360** may be processed to generate a global contour map indicating the amount of material to be removed as a function of two-dimensional position on the wafer. The material is then removed in accordance with the contour map using the selective material removal tool.

At **1370**, local frequency tuning may be performed in addition to, or instead of, the global frequency tuning performed at **1365**. "Local" frequency tuning is performed with a spatial resolution smaller than an individual filter device. The test results from **1360** may be processed to generate a map indicating the amount of material to be removed at each filter device. Local frequency tuning may require the use of a mask to restrict the size of the areas from which material is removed. For example, a first mask may be used to restrict tuning to only shunt resonators, and a second mask may be subsequently used to restrict tuning to only series resonators (or vice versa). This would allow independent tuning of the lower band edge (by tuning shunt resonators) and upper band edge (by tuning series resonators) of the filter devices.

After frequency tuning at **1365** and/or **1370**, the filter device is completed at **1375**. Actions that may occur at **1375** include forming bonding pads or solder bumps or other means for making connection between the device and external circuitry (if such pads were not formed at **1345**); excising individual filter devices from a wafer containing multiple filter devices; other packaging steps; and additional testing. After each filter device is completed, the process ends at **1395**.

Closing Comments

Throughout this description, the embodiments and examples shown should be considered as exemplars, rather than limitations on the apparatus and procedures disclosed or claimed. Although many of the examples presented herein involve specific combinations of method acts or system elements, it should be understood that those acts and those elements may be combined in other ways to accomplish the same objectives. With regard to flowcharts, additional and fewer steps may be taken, and the steps as shown may be combined or further refined to achieve the methods described herein. Acts, elements and features discussed only in connection with one embodiment are not intended to be excluded from a similar role in other embodiments.

As used herein, "plurality" means two or more. As used herein, a "set" of items may include one or more of such items. As used herein, whether in the written description or the claims, the terms "comprising", "including", "carrying", "having", "containing", "involving", and the like are to be understood to be open-ended, i.e., to mean including but not limited to. Only the transitional phrases "consisting of" and "consisting essentially of", respectively, are closed or semi-closed transitional phrases with respect to claims. Use of ordinal terms such as "first", "second", "third", etc., in the claims to modify a claim element does not by itself connote any priority, precedence, or order of one claim element over another or the temporal order in which acts of a method are performed, but are used merely as labels to distinguish one claim element having a certain name from another element having a same name (but for use of the ordinal term) to distinguish the claim elements. As used herein, "and/or" means that the listed items are alternatives, but the alternatives also include any combination of the listed items.

It is claimed:

1. An acoustic resonator device comprising:

a piezoelectric plate; and

a conductor pattern formed on a surface of the piezoelectric plate, the conductor pattern comprising:

an interdigital transducer (IDT) comprising a first busbar, a second busbar, and n interleaved parallel fingers, where n is a positive integer, wherein the fingers extend alternately from the first and second busbars, and the fingers include a first finger and an n'th finger at opposing ends of the IDT;

a first reflector element proximate and parallel to the first finger; and

a second reflector element proximate and parallel to the n'th finger, wherein

a center-to-center distance pr between the first reflector element and the first finger and between the second reflector element and the n'th finger is greater than or equal to 1.2 times a pitch p of the IDT and less than or equal to 1.5 times the pitch p.

2. The device of claim **1**, the conductor pattern further comprising:

a third reflector element proximate and parallel to the first reflector element, wherein the first reflector element is between the third reflector element and the first finger; and

a fourth reflector element proximate and parallel to the second reflector element, wherein the second reflector element is between the fourth reflector element and the n'th finger.

3. The device of claim **2**, wherein

a width mr of the first, second, third, and fourth reflector elements is configured to increase a Q-factor of the device at a predetermined frequency.

4. The device of claim **3**, wherein

the device is a shunt resonator in a ladder bandpass filter circuit having a passband, and

mr is selected to increase a Q-factor of the device at a lower edge of the passband.

5. The device of claim **3**, wherein

the device is a series resonator in a ladder bandpass filter circuit having a passband, and

mr is selected to increase a Q-factor of the device at an upper edge of the passband.

6. The device of claim **2**, wherein

the first and third reflector elements and the first finger are connected to a same one of the first and second busbar, and

the second and fourth reflector elements and the n'th finger are connected to a same one of the first and second busbar.

7. The device of claim **2**, wherein

the first and third reflector elements are connected to each other and capacitively coupled to the first finger, and

the second and fourth reflector elements are connected to each other and capacitively coupled to the n'th finger.

8. The device of claim **2**, wherein

a center-to-center distance between the first and third reflector elements and a center-to-center distance between the second and fourth reflector elements are equal to pr.

9. The device of claim **1**, wherein

a width mr of the first and second reflector elements is configured to increase a Q-factor of the device at a predetermined frequency.

10. The device of claim **9**, wherein

the device is a shunt resonator in a ladder bandpass filter circuit having a passband, and

mr is selected to increase a Q-factor of the device at a lower edge of the passband.

11. The device of claim **9**, wherein

the device is a series resonator in a ladder bandpass filter circuit having a passband, and

mr is selected to increase a Q-factor of the device at an upper edge of the passband.

12. The device of claim **1**, wherein

when an RF signal is applied between the first and second busbars, the first reflector element is at substantially the same potential as the first finger and the second reflector element is at substantially the same potential as the n'th finger.

13. The device of claim **12**, wherein

the first reflector element and the first finger are connected to a same one of the first and second busbar, and

the second reflector element and the n'th finger are connected to a same one of the first and second busbar.

14. The device of claim **12**, wherein

the first reflector element is capacitively coupled to the first finger, and

the second reflector element is capacitively coupled to the n'th finger.

15. An acoustic resonator device comprising:

a substrate;

a piezoelectric plate, a portion of the piezoelectric plate forming a diaphragm spanning a cavity in the substrate; and

a conductor pattern on a surface of the piezoelectric plate, the conductor pattern comprising:

an interdigital transducer (IDT) including a first busbar, a second busbar, and n interleaved parallel fingers, where n is a positive integer, wherein the fingers extend alternately from the first and second busbars, and the fingers include a first finger and an n'th finger at opposing ends of the IDT;

a first reflector element proximate and parallel to the first finger; and

a second reflector element proximate and parallel to the n'th finger, wherein

the n interleaved parallel fingers, the first reflector element, and the second reflector element are on the diaphragm, and

a center-to-center distance pr between the first reflector element and the first finger and between the second reflector element and the n'th finger is greater than or equal to 1.2 times a pitch p of the IDT and less than or equal to 1.5 times the pitch p.

16. The device of claim **15**, wherein

a width mr of the first and second reflector elements is configured to increase a Q-factor of the device at a predetermined frequency.

17. The device of claim **15**, the conductor pattern further comprising:

a third reflector element proximate and parallel to the first reflector element, wherein the first reflector element is centered between the third reflector element and the first finger; and

a fourth reflector element proximate and parallel to the second reflector element, wherein the second reflector element is centered between the fourth reflector element and the n'th finger, wherein

the third and fourth reflector elements are on the diaphragm.

* * * * *